Phase 1 Integrated Systems Test and Characterization Report for the 5-Megawatt Dynamometer and Controllable Grid Interface

Scott Lambert, Vahan Gevorgian, Scott Dana, and Robb Wallen
National Renewable Energy Laboratory

NREL is a national laboratory of the U.S. Department of Energy
Office of Energy Efficiency & Renewable Energy
Operated by the Alliance for Sustainable Energy, LLC

This report is available at no cost from the National Renewable Energy Laboratory (NREL) at www.nrel.gov/publications.

Technical Report
NREL/TP-5000-63073
March 2018

Contract No. DE-AC36-08GO28308

NREL
NATIONAL RENEWABLE ENERGY LABORATORY

Phase 1 Integrated Systems Test and Characterization Report for the 5-Megawatt Dynamometer and Controllable Grid Interface

Scott Lambert, Vahan Gevorgian, Scott Dana, and Robb Wallen
National Renewable Energy Laboratory

Suggested Citation
Lambert, Scott, Vahan Gevorgian, Scott Dana, and Robb Wallen. 2018. *Phase 1 Integrated Systems Test and Characterization Report for the 5-Megawatt Dynamometer and Controllable Grid Interface*. Golden, CO: National Renewable Energy Laboratory. NREL/TP-5000-63073. www.nrel.gov/docs/fy18osti/63073.

National Renewable Energy Laboratory
15013 Denver West Parkway
Golden, CO 80401
303-275-3000 • www.nrel.gov

Technical Report
NREL/TP-5000-63073
March 2018

Contract No. DE-AC36-08GO28308

NOTICE

This report is available at no cost from the National Renewable Energy Laboratory (NREL) at www.nrel.gov/publications.

Available electronically at SciTech Connect http:/www.osti.gov/scitech

Available for a processing fee to U.S. Department of Energy and its contractors, in paper, from:

U.S. Department of Energy
Office of Scientific and Technical Information
P.O. Box 62
Oak Ridge, TN 37831-0062
OSTI http://www.osti.gov
Phone: 865.576.8401
Fax: 865.576.5728
Email: reports@osti.gov

Available for sale to the public, in paper, from:

U.S. Department of Commerce
National Technical Information Service
5301 Shawnee Road
Alexandria, VA 22312
NTIS http://www.ntis.gov
Phone: 800.553.6847 or 703.605.6000
Fax: 703.605.6900
Email: orders@ntis.gov

Cover Photos by Dennis Schroeder: (left to right) NREL 26173, NREL 18302, NREL 19758, NREL 29642, NREL 19795.

NREL prints on paper that contains recycled content.

Table of Contents

List of Figures

List of Tables

1 Objective

This report details the commissioning of the 5-MW dynamometer and Controllable Grid Interface (CGI) at the National Wind Technology Center (NWTC) at the National Renewable Energy Laboratory (NREL). The purpose of these characterization tests was to verify the dynamometers performance over the widest possible range of operating conditions, verify interconnection with and fault generation capability of the CGI, gain insight into system-level behavior, and establish confidence in measurement data.

2 Background

The 5-MW dynamometer at the NWTC is primarily designed to reproduce the input forces and electrical grid conditions that a wind turbine experiences in the field, but conducted in a controlled laboratory environment. To accomplish this, two unique pieces of equipment are employed:

- Drive system with nontorque loading (NTL) capability
- Controllable grid interface (CGI).

Figure 1 shows the dynamometer driveline and its primary components. A 6-MW induction motor and variable frequency drive (VFD) are used to drive a three-stage speed reducing gearbox. The low-speed shaft (LSS) transmits torque to the NTL system via two large crowned tooth couplings that allow misalignment between the gearbox and NTL system. The NTL device uses hydraulic actuators to apply loads in five of the six degrees of freedom to a nacelle at the rotor interface. Dynamometer drive torque is allowed to pass through the machine nearly without friction by use of hydrostatic bearings. The machine is capable of simulating the large pitch and yaw moments that are caused by uneven wind forces on wind turbine rotors and provides thrust load capability in addition to lateral and downward forces.

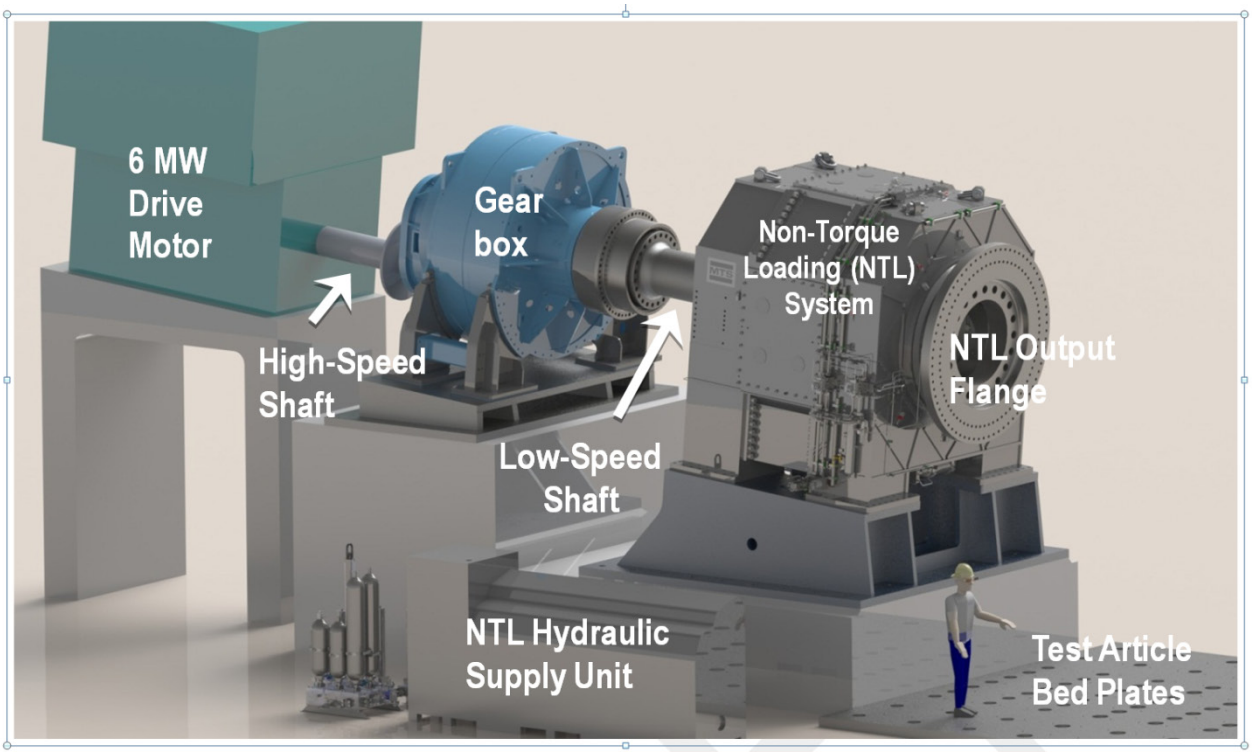

Figure 1. NREL's dynamometer drive system

The specifications for the 5-MW dynamometer are listed in Table 1.

Table 1. NWTC Dynamometer Specifications

Characteristic	Specification
Torque/Speed	0–12 revolutions per minute (rpm): torque limited to 4.6 meganewton meters (MNm) (40,000,000 in pounds [lbs]) 12–24 rpm: power limited to 5.8 MW continuous, 6.4 MW for 1 minute Bidirectional rotation Full regeneration (can absorb 6 MW from test article)
Yaw and Pitch Moments	± 7.2 MNm (64,000,000 lbs)
Thrust Force	± 4 meganewtons (MN) (900,000 lbs)
Radial Force	± 3.25 MN (730,000 lbs)
Test Article Size Limits	20 x 6 meters (m) (65 x 20 feet [ft]) test article footprint Six,1 x 9.8 m (20 x 32 ft) steel floor with 198 M36 threaded holes to connect test article to floor
Test Article Handling	Two 75-ton cranes 14 m (45 ft) maximum hook height 143-ton (net capacity) spreader bar for single point lifts Door that is 6.7 m (22 ft) wide and 9.1 m (30 ft) high Drive-through high bay for trucks of unlimited length
Test Article Grid Connection	13,200–690 volts alternating current, 3 megavolts ampere (MVA) transformer Indoor pad for custom transformer to 13.2 kilovolts ampere, 60-hertz grid Controllable grid interface connection available
Test Article Driveline Connection	Inclination: 5° fixed Output flange center height: 4 m (13.1 ft) Output flange outer bolt circle 2.3 m (91 in) diameter, 72 M42 threaded holes Output flange inner bolt circle: 2.0 m (79 in) diameter, 54 M48 threaded holes
Cooling/Heating	850 m^3/minute (30,000 ACFM) forced ventilation with outside air (6,081 ft elevation) Gas heat for periods of no operation Climate-controlled control room
Control System	Torque and speed control modes Ramp operation, arbitrary time series, and external command capability 350-hertz update rate Custom scripting and programming
Data Acquisition	500+ channel, 24 bit, distributed data acquisition system Standalone power quality condition monitoring system meeting International Electrotechnical Commission 61400-21 requirements

The NWTC's 7-megavolt ampere (MVA) CGI (or "grid simulator") facility (shown in Figure 2) tests wind, solar, energy storage devices, and other renewable energy technologies in a utility-scale grid environment. It also allows manufacturers and system operators to assess many aspects of grid integration and provides hardware-in-the-loop capability combined with NWTC dynamometers, actual utility-scale wind and solar generators, and energy storage components. In addition, the CGI can emulate various grid disturbances and estimate impacts of generation response on the grid. Ultimately, it is a unique platform for testing many advanced "grid-friendly" controls for renewables.

Figure 2. NREL's controllable grid interface (CGI). ***Photo by Mark McDade, NREL***

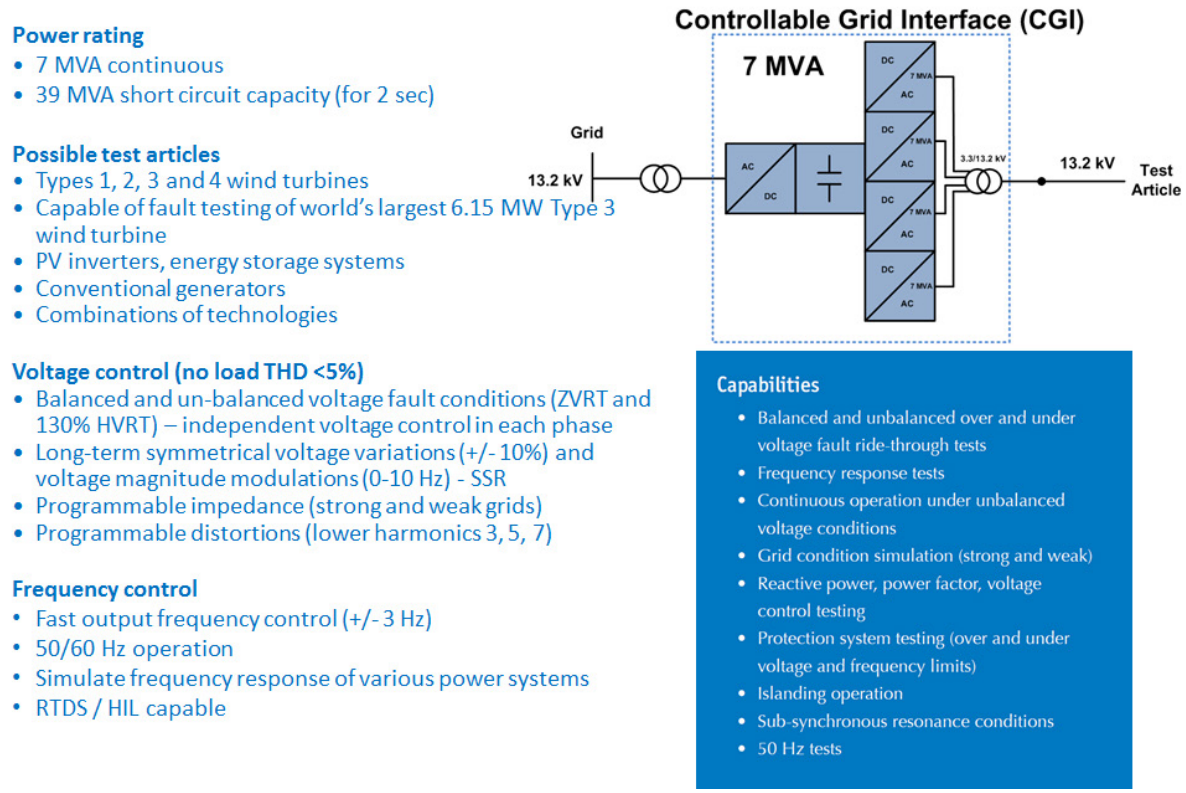

Figure 3. CGI specifications

The CGI's electrical topology is based on ABB's ACS6000 variable frequency drive power converter blocks that are combined together. Regarding test articles, four ACS6000 active inverters are combined in parallel to provide sufficient short-circuit current capability, which is an important feature when testing wind turbine generators that have their stator windings directly coupled with the power grid (Types 1, 2, and 3 wind turbines). The inverters are connected to a custom-made 7-MVA power transformer with six windings that are combined in parallel and series manner on the low- and high-voltage sides, respectively. This unique transformer

configuration allows for four-wire operation (three phases and neutral) and independent control of each phase voltage. As a result, any desired voltage fault scenario (under and overvoltage, symmetrical, or nonsymmetrical) can be achieved.

2.1 Interfaces

A test specimen interfaces with the dynamometer facility in several areas:

- **Rotor or main shaft flange**. The shaft adapter connects the test drivetrain's main shaft to the NTL output flange nominally 4 meters above to dyno floor. This disk-like adapter transmits torque and nontorque loads to the test drivetrain.
- **Foundation or tower substitute**. The test stand connects the test drivetrain to the floor and foundation in a manner similar to the turbine's tower with the exception that the test stand is only 2.1 meters (m), or 7 feet, tall. The stand is bolted to the dynamometer floor using 52 M36 bolts Cementatious grout with a nominal thickness of 100 millimeters (mm) is used to accommodate alignment in pitch and height, and oversized, 76-mm diameter holes help align the test article in yaw, axial, and lateral directions.
- **Grid electrical, instrumentation, and controls**. The grid electrical connection is made via a 3-MVA delta-wye transformer, which converts 13,200 volts (V) of power from the NWTC grid to 690 V power for the test drivetrain's power electronics. A circuit breaker with circuit protection sensors provides a disconnect point for the test drivetrain inside the dynamometer high bay. The power electronic equipment used to convert the generator power to 690 V is connected to and controlled by the NREL dynamometer's real-time controller.
    - Signals from the test article and dynamometer drive systems, such as temperatures, pressures, and displacements, are connected to the NREL data acquisition real-time controller. Two rotating data acquisition modules attached to the low-speed shafting provide torque, main shaft bending, and coupling displacement data. All of the signals system-wide are then shared over a reflective memory system (Scram-net) and available for viewing or further processing.
- **Heat rejection and building systems**. The test drivetrain gearbox and permanent-magnet generator are cooled using oil-to-air and air-to-air forced-convection heat exchangers mounted in the nacelle. The power electronics for the turbine under test are liquid cooled by a glycol-to-air, forced-convection, heat exchanger located on the high bay floor. Building ventilation removes the hot exhaust from the heat exchangers via vents close to the dynamometer roof.

2.2 Coordinate System

NREL uses the following International Standards Organization 61400-1 standard coordinate system in the dynamometer to define loading conditions at the test specimen rotor flange (shown in Figure 4).

Fx = thrust force

Fy = lateral force
Fz = upward force
Mx = main shaft moment or torque
My = pitch moment
Mz = yaw moment

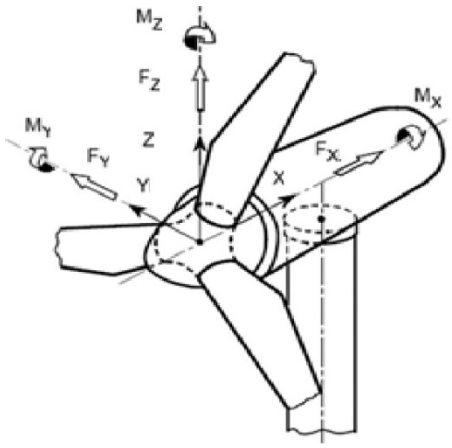

Figure 4. Test specimen coordinate system

For test loads, the torque load and NTLs are aligned with the LSS on the dynamometer. This configuration is consistent with the common wind turbine drivetrain practice as described below.

- The origin is at the center of the test drivetrain's main shaft flange that connects to the rotor.
- The X-axis is aligned with the input LSS with the downwind direction being positive. In the NWTC's 5-MW dynamometer, this axis is inclined at 5° to the horizontal. Thrust (Fx) is the force acting along the positive X-axis and torque is a moment about the X-axis.
- The Z-axis is orthogonal to the X-axis with upward being positive. The upward force acts along the Z-axis and the yaw moment (Mzz) acts about the Z-axis. (The term, "upward" is used rather than "vertical" because the NTLs are oriented along the axis of the LSS, which is inclined at 5° from horizontal. Therefore, upward loads are tilted 5° from vertical.)

- The Y-axis is orthogonal to the X-axis and Z-axis with leftward being positive when viewing the drivetrain from upwind. The lateral force acts along the Y-axis and rotor weight causes a negative pitch moment (Myy) about the Y-axis.
- The rotor azimuth angle increases clockwise when viewed from upwind with 0° being upward. Normal rotor rotation in the test drivetrain, as for most wind turbines, is positive.

2.3 General Dynamometer Test Procedures

Dynamometer characterization testing thus far has been conducted in a sequence that permits verification of safety features and controls to reduce the risk of overloading the test drivetrain. Basic system control and safety have been verified and safety limits for the NTL have been established.

During characterization testing, NREL followed the start-up and shutdown procedure outlined below, which provides the opportunity to check data acquisition integrity and compile data sets under unloaded and low load conditions. Procedure steps include:

- Assigning roles and responsibilities to dynamometer team members
- Recording all significant events, settings, and file locations in the dynamometer logbook
- Verifying maximum load, speed, and displacement settings appropriate for the next test sequence
- Clearing dynamometer high bay, placing warning signs, and turning on warning lights
- Turning off high bay heaters and turning on high bay air handler(s) (if required)
- Starting to acquire data before operating the motor and NTL, which ensures that the data will capture all normal and any unexpected events during start-up and testing
- Continuing to acquire data during testing except what may be required for specific test sequences; this includes commanding the NTL to apply tare loads to minimize all loads on the main shaft of the test drivetrain, then beginning the slow rotation of the test drivetrain. Stopping data acquisition upon completion of testing and shut down of the variable frequency drive (VFD) and NTL

2.4 Dynamometer Control System

The 5-MW dynamometer control system is comprised of the following three systems:

- The **high-level control system** provides real-time control of speed and torque of the dynamometer drive and the NTL system. Both the dynamometer VFD and NTL systems feature their own specific control systems that monitor and control each of those pieces of equipment. A master computer coordinates between the two systems and is the primary interface that the dynamometer operator uses to command desired test conditions. This system is flexible, modular, and easily extensible using off-the-shelf hardware.
- The **facility programmable logic controller (PLC) system** monitors the health of all the dynamometer systems used during testing, detects and commands appropriate system responses to faults, and provides an operator overview of all dynamometer functions. The PLC coding is thoroughly tested and revision-controlled. It cannot be changed during

testing by the dynamometer operator, which protects against accidental or intentional degradation of the facility and ensures personnel safety.

- The **fault/shutdown system** is largely hard-wired to minimize system response to critical faults. Through this system, equipment fault or dynamometer personnel can initiate either of two dynamometer shutdown procedures: emergency shutdown or emergency power-off. This system is also used to lock out the dynamometer's VFD and nontorque systems so that personnel can safely access the dynamometer and test drivetrains for nonelectrical-related inspections and work.
    - An emergency shutdown initiates a controlled "process stop" on the drive, NTL, and test drivetrain to quickly remove kinetic energy from the system. The VFD applies braking torque to the dynamometer and test drivetrains to bring rotating equipment to a stop within 1 minute. The NTL aborts the test sequence and locks the actuators to hold position and load. The test drivetrain is disconnected from the grid to ensure that its generator does not "motor" the drivetrain. This shutdown mode is not harmful to the dynamometer or test drivetrain equipment and can be commanded by support personnel as well as the dynamometer operator whenever any abnormal behavior is observed. Once the driveline has been stopped and the dynamometer team has assessed the situation, the operator can manually command the NTL to a zero or low-load condition as appropriate.
    - An emergency power-off system responds to the fire alarm monitors and "pull stations" located throughout the dynamometer facility. In case of fire, it opens the large electrical contactors that provide power to the dynamometer VFD and test drivetrain generator. If this system is activated, or if there is a power outage, the dynamometer motor cannot be used as a brake to stop rotation. So a mechanical disk brake on the dynamometer's high-speed shaft (HSS) assembly is used to stop the driveline. The emergency power-off system also activates the fire alarm klaxons and summons the local fire department.

Select signals from the control system are recorded and become part of the permanent record of dynamometer operations. In addition, any of the signals processed through the control system may be monitored and recorded by the data acquisition system as needed.

Prior to the first start of the dynamometer for this work, NREL verified the operation of each fault sensor to ensure that the fault was detected at the dynamometer facility PLC control panel and that the proper, emergency shutdown signal was sent to the dynamometer VFD to shut it down. The following faults were verified by simulating the fault signal to the facility PLC:

- Dynamometer motor overspeed
- NTL fault
- Dynamometer gearbox lube oil pressure too low
- Dynamometer gearbox HSS bearing temperature too high
- Test drivetrain controller fault.

2.5 Data Acquisition System

The dynamometer has a distributed data acquisition system (DAS) based on National Instruments deterministic Ethernet platform [1]. This architecture permits conversion of analog signals to noise-immune, digital signals at several locations throughout the dynamometer, including on the rotating low-speed shaft. The signals are transmitted in digital form by fiber optic cabling to the primary data acquisition computer adjacent to the dynamometer's control room. Control, monitoring, and data recording are located adjacent to the control room in a protected and temperature-controlled environment.

Two analog-to-digital systems are mounted to the dynamometer's LSS— one between the gearbox and NTL system and one between the NTL system and the test drivetrain. The digital outputs of those systems are transmitted across a two-channel, fiber-optic rotary joint to the nonrotating frame. Another analog-to-digital system is located on or near the test drivetrain. As noted earlier, other system control signals are connected to the DAS for monitoring and recording.

Appendix A contains a listing of sensors and resulting signals used to monitor dynamometer operating conditions.

2.6 Other Measurements

The dynamometer's VFD provides a variety of direct and calculated channels of data useful for commissioning tests. Of these, motor speed, current, power, and torque were recorded and reported. Motor speed is provided by an encoder mounted on the motor's shaft. Current is provided by current transducers located on connections between the VFD and the motor. Power is calculated from current and voltage measurements on the connections between the VFD and the motor, and torque is calculated from current measurements and various motor parameters. These channels can be used as additional comparisons with the primary measurements described earlier.

The test drivetrain was equipped with an LSS encoder and its signal was recorded and compared to the measurements available from the dynamometer's low speed shaft and motor. In addition, a power meter indicates real and reactive power at the connection of the generator to the grid.

3 Dynamometer Driveline Characterization

Torque and rotational speed in the dynamometer driveline are controlled using an ABB variable frequency drive. The bidirectional and regenerating capability of the drive and motor permit operation in both directions of shaft rotation and power flow. The dynamometer can be operated in either torque control, speed control, or a combination of the two modes. In torque control, the operator commands a torque level that the dynamometer motor applies while the test drivetrain regulates speed. In this scenario, if the test specimen cannot provide the torque required to prevent acceleration, there is potential for the dynamometer to over speed. In speed control, the dynamometer operator commands the motor's speed, and torque is dictated by the test drivetrain's torque speed characteristics.

Figure 5 shows the torque, speed, and power operating envelope for the dynamometer. The areas under the constant power curves are made possible by field weakening.

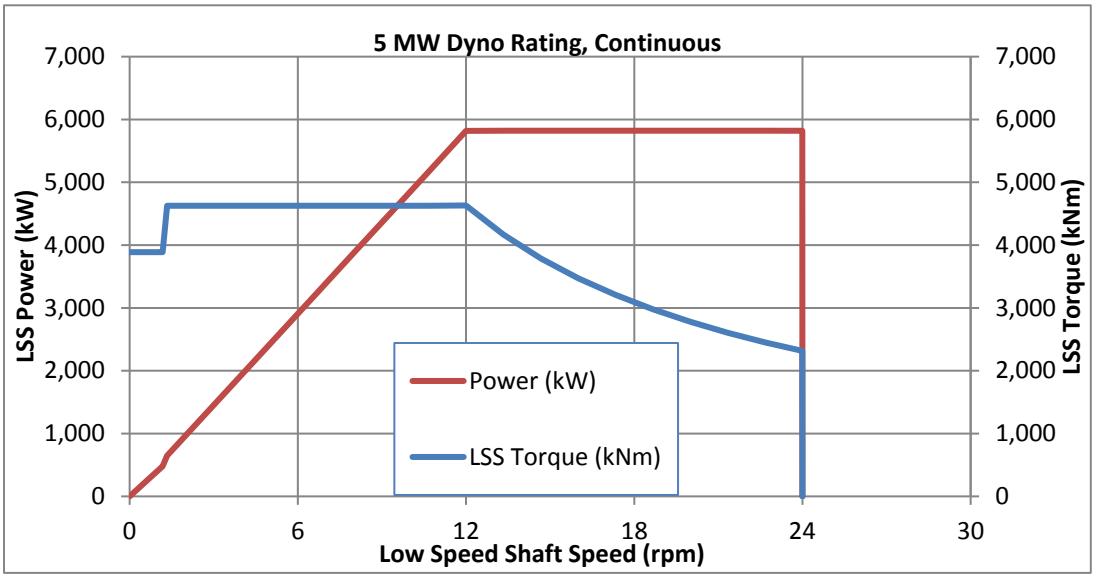

Figure 5. Dynamometer torque and power versus speed

Figure 6 demonstrates the dynamometer's operating characteristics in speed control mode. For this test case, the dynamometer speed was commanded to be 13 revolutions per minute (rpm) at the LSS. As torque was stepped up and back down the speed was held constant. In Figure 6, the measured torque from the torque spool is plotted in green along with a calculation of the motor air gap torque performed by the VFD and the speed feedback is plotted in red. At each torque step there is a momentary increase in the feedback signal. This difference between the command and actual speed is used to drive the speed to the desired value.

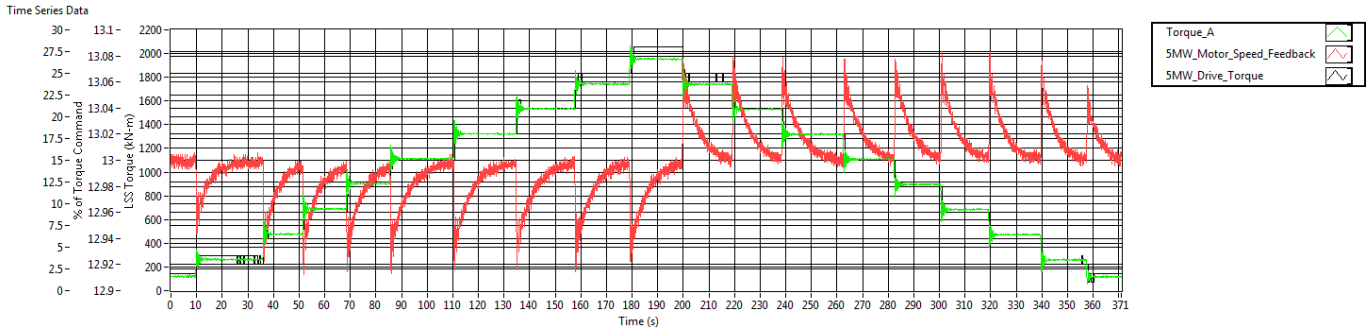

Figure 6. Dynamometer in speed control

3.1 Torque

The primary measurement of torque applied to the test drivetrain was provided by a custom torque transducer located on the dynamometer's LSS between the gearbox and NTL system. This torque transducer features a small diameter section that is precisely shaped to provide a good strain response to torque. The gaged area of the transducer features two full bridge sets of strain gages in which each bridge set consists of 16 gages located at 22.5° intervals around the transducer's outer circumference. The torque transducer was calibrated on a custom stand mounted on the 5-MW dynamometer's steel floor.

A Himmelstien Model MCRT87008V torque transducer was incorporated into the HSS of the dynamometer. This instrument provides a measurement that can be used to directly measure both motor and braking torque. Measurements at both the input and output stages of the gearbox allow efficiency estimates to be made and may provide a convenient method for long-term condition monitoring of the gearbox to be performed.

Figure 7 shows the torque signals from the two channels on the LSS transducer and the HSS torque transducer during two step changes in the commanded torque. The step changes in torque along with backlash in the gearbox and couplings, shaft stiffness, and rotational inertia produce a damped oscillation in the driveline as seen in the plot.

From the plot it can be seen how closely the two channels (A and B) on the torque transducer agree.

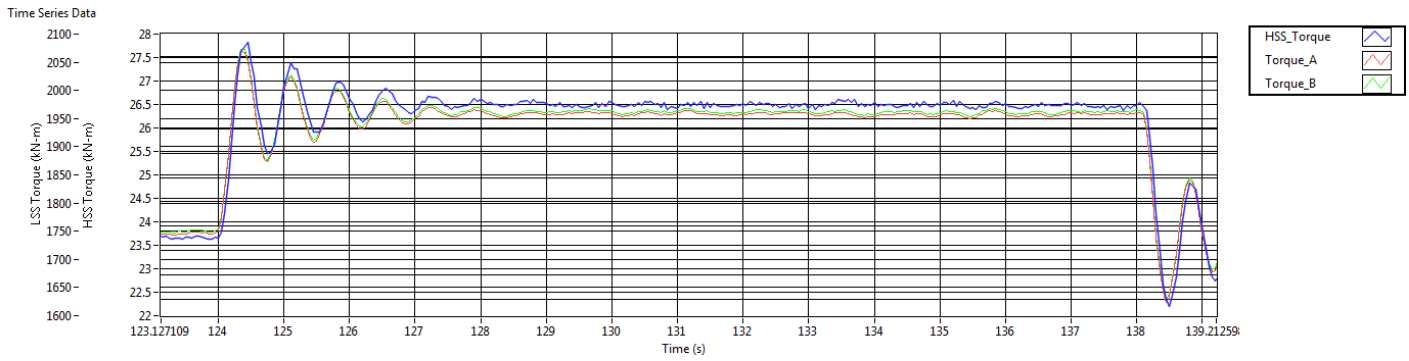

Figure 7. Torque response of LSS and HSS

As seen in Figure 8, performing a fast Fourier transform (FFT) on these signals reveals the dominate frequency of the oscillations at 1.4 Hz.

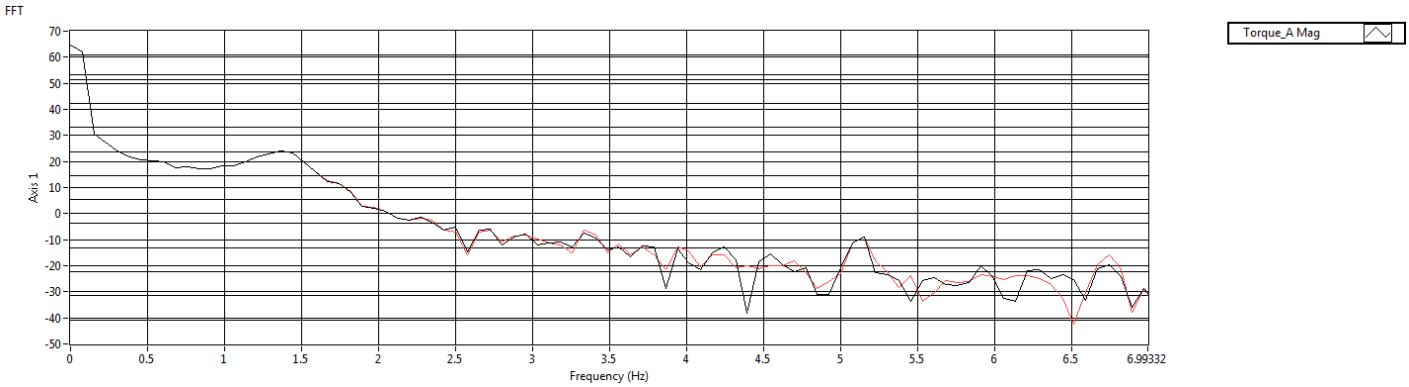

Figure 8. Frequency content of dynamometer drive torque

Table 2. 5-MW Dynamometer Gearbox Gear Ratio Data

Component	# of teeth	Ratio
Third-stage ring	127	6.521739
Third-stage planet	51	
Third-stage sun	23	
Second-stage ring	131	6.240
Second-stage planet	53	
Second-stage sun	25	
First-stage gear	91	1.857143
First-stage pinion	49	
Total Ratio	N/A	75.57764

3.2 Driveline Efficiency

Shaft power delivered to the test drivetrain is reduced by friction in the gearbox. Gear mesh friction and bearing rolling friction create heat that needs to be transferred effectively to maintain acceptable operating conditions.

An estimate of gearbox efficiency is shown in Figure 9 for the time series data in Figure 6. The overall gearbox efficiency tends to improve as torque increases, which may be a result of the microgeometry of the gear teeth being optimized for higher torque and power levels.

The primary means of heat rejection for the gearbox is through the pressure feed oil system. An oil-to-glycol heat exchanger is used to cool the system reservoir and return the oil used to feed the gearbox. The large capacity of the oil reservoir and subsequent thermal mass require high-power, long-duration run times to prove out the cooling system. These estimates provide some

assurance that the cooling system for the gearbox will be sufficient, given that it was sized for 97% gearbox efficiency at 5 MW of power throughput.

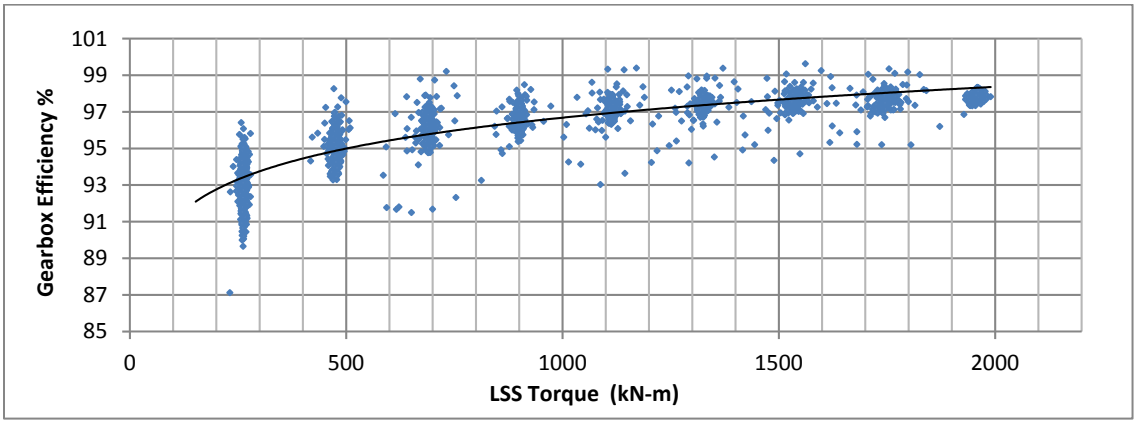

Figure 9. Estimated efficiency of dynamometer gearbox

3.3 High-Speed-Shaft Torque Limiter

A mechanical torque limiting device built into the HSS is attached to the output of the drive motor. This device prevents the dynamometer from inducing excessive torque loads from a motor fault, test specimen fault, or other unusual transient condition. The torque limiter consists of five modules that can be engaged individually or adjusted to a lower setting if the maximum desired torque during testing is limited. In its default configuration, the torque limiter has been adjusted to limit torque to 87.5 kNm (114% of the gearbox's rated momentary torque).

NREL engineers tested the HSS torque limiting device by engaging a single module while leaving the remaining four modules disengaged, and then gradually increased the torque command until the device was activated. Figure 10 shows a single module trip event.

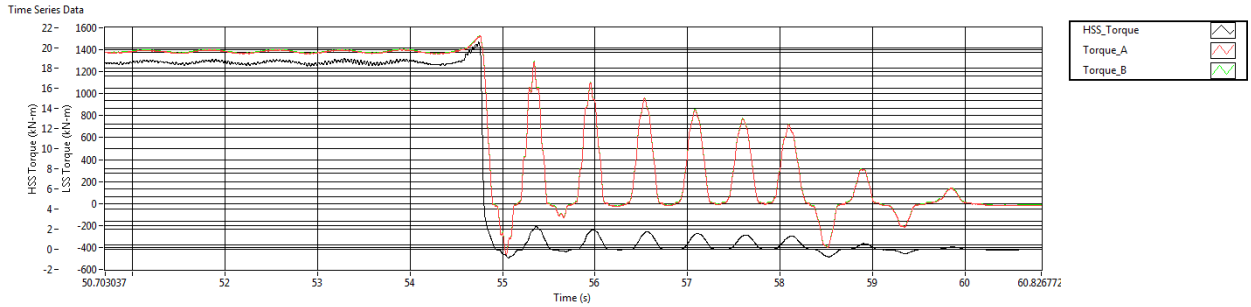

Figure 10. Dynamometer torque during limiting event

3.4 High-Speed Shaft Brake

Whenever possible, the dynamometer drive motor is used to bring the driveline from its operating speed to zero rpm. A brake assembly built into the HSS is activated in the event of a power outage to bring the driveline to a stop before hydraulic bearing pressure in the NTL system is lost and subsequent damage is done.

Figure 11 shows the time history of the HSS and LSS torque during a braking event. After a small increase in torque was commanded, the test specimen trips off line and the brake is

activated. LSS torque quickly reversed direction and remained negative throughout the event. HSS torque remained positive as a result of the drive motor inertia.

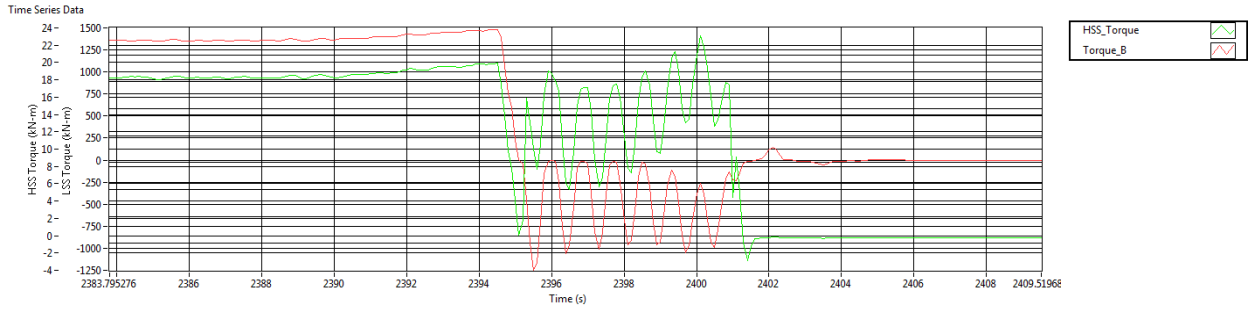

Figure 11. Emergency stop with HSS brake

3.4.1 Dynamometer Speed/Azimuth Position

The primary measurement of the main shaft speed and azimuth is provided by a shaft encoder mounted on the upwind end of the gearbox that connects to the low-speed output shaft of the gearbox. A pulse counter/timer circuit derives the speed, giving a 0- to 5-volt DC (VDC) output proportional to speed. The azimuth angle is obtained from a separate counter circuit using the same encoder input, generating a 0–4.095 VDC saw tooth output proportional to the shaft position. The saw tooth is reset to zero by the index pulse once per revolution. Resolution is about 1/4°.

Figure 12 shows a speed sweep from 0 rpm up to 13 rpm and back to zero. The torque applied is kept to a minimum by accelerating the driveline in a gentle ramp and then coasting down. The test specimen is kept disconnected from the grid power. The red saw tooth wave form is the output from the LSS encoder.

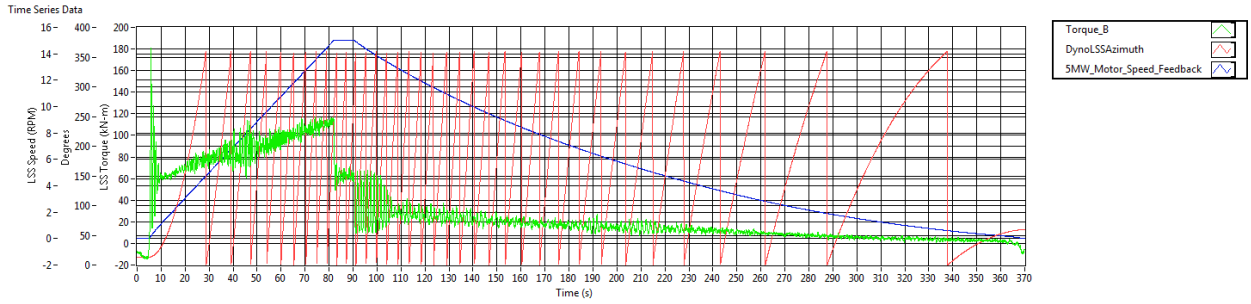

Figure 12. Dynamometer speed, azimuthal position, and torque

3.5 Torsional Deflection and Backlash

Torsional deflection or “windup” and backlash in the driveline cause several undesirable effects. Because the torsional stiffness and rotational mass of the system determine the torsional modes, resonant frequencies, and dynamic response capabilities, it is desirable to have a light yet stiff system to avoid low-frequency oscillations, improve controllability, and increase dynamic response. Backlash in the driveline can introduce a delay between command and response that can excite ringing and introduce undesirable shock loads. An accurate measurement of the LSS and gearbox torsional stiffness is important to validate dynamic models and enable advanced testing methods, such as reproduction of field conditions or model-in-the-loop testing.

To characterize the LSS stiffness, a calculated channel was created that compares the LSS encoder signal to an encoder on the test specimen gearbox. Figure 13 shows the output of this calculation and the operating torque. Although there is a significant amount of noise in the calculation, probably as a result of run out in one or both of the encoders, we can get an approximation of torsional deflection. The calculated stiffness values of .00028 degrees per kNm will be compared to dynamics models for tuning and validation in future characterization testing.

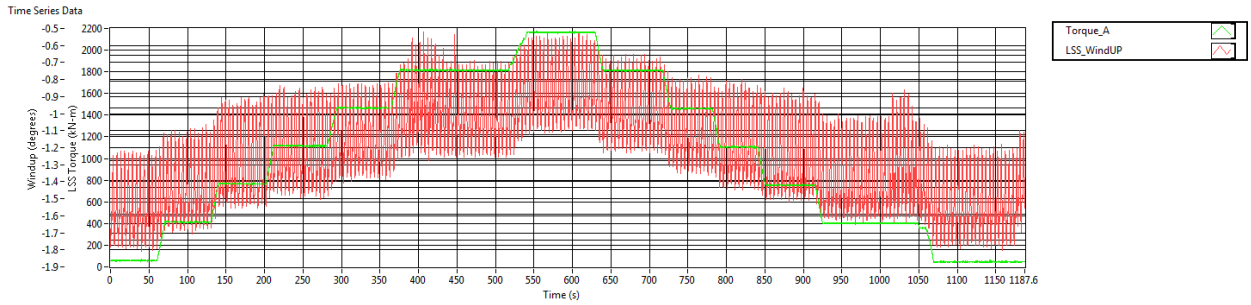

Figure 13. Dynamometer driveshaft windup

3.6 Low-Speed-Shaft Loads and Displacements

Flexible couplings in the dynamometer's LSS assembly allow axial, radial, and angular misalignment of the NTL rotor relative to the gearbox output shaft. Whenever torque is applied, any misalignment in these couplings will induce thrust, bending moments, and radial loads. Moments induced by the downwind coupling add to or subtract from the moments applied by the NTL device to the test drivetrain. Moments induced by the upwind coupling are reacted by the dynamometer gearbox. Resistance to changes in the axial position of the shafting creates forces that add to the thrust force applied by the NTL system. Therefore, it is important to quantify these loads and displacements to fully understand the loads applied during testing.

NREL has noted this behavior with nontorque loads during testing in the U.S. Department of Energy-sponsored Gearbox Reliability Collaborative initiative and in testing for private wind turbine companies. This experience suggests that coupling loads may be predicted using measurements of LSS torque and the magnitude and direction of each coupling's alignment. NREL has instrumented the LSS assembly with strain gages and displacement transducers to characterize and account for these loads.

Two strain-gage bridges measure bending loads at each end of the LSS assembly. The pair of bridges measure bending in two orthogonal planes. The bridge with gages located at the 0° and 180° positions measure bending about the rotating Y-axis. When multiplied by the sine of the azimuth angle, this signal indicates a moment about the nonrotating Z-axis. When multiplied by the cosine of the azimuth angle, this signal indicates a moment about the nonrotating Y-axis.

Similarly, the bridge with gages located at the 90° and 270° positions yield yaw and pitch moment measurements when multiplied by the sine and cosine of the azimuth angle plus 90°, respectively.

Each of the two flexible couplings in the LSS assembly feature two proximity sensors. In combination with the azimuth angle measurement, these sensors define the coupling angular alignment vector and axial alignment position.

Figure 14shows the bending signals obtained from the six strain gage channels on the LSS during a coast down. Coast down data was used so that the effect of torque can be eliminated and the static offsets can be determined.

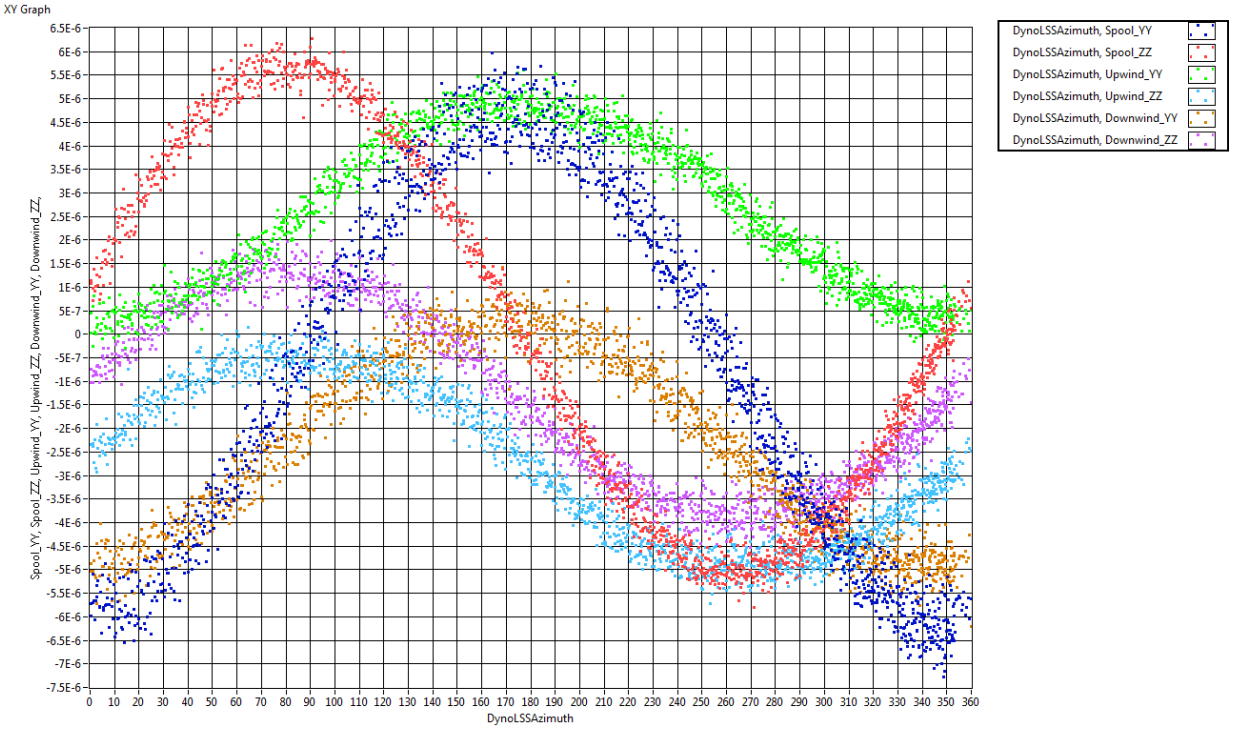

Figure 14. LSS bending signals

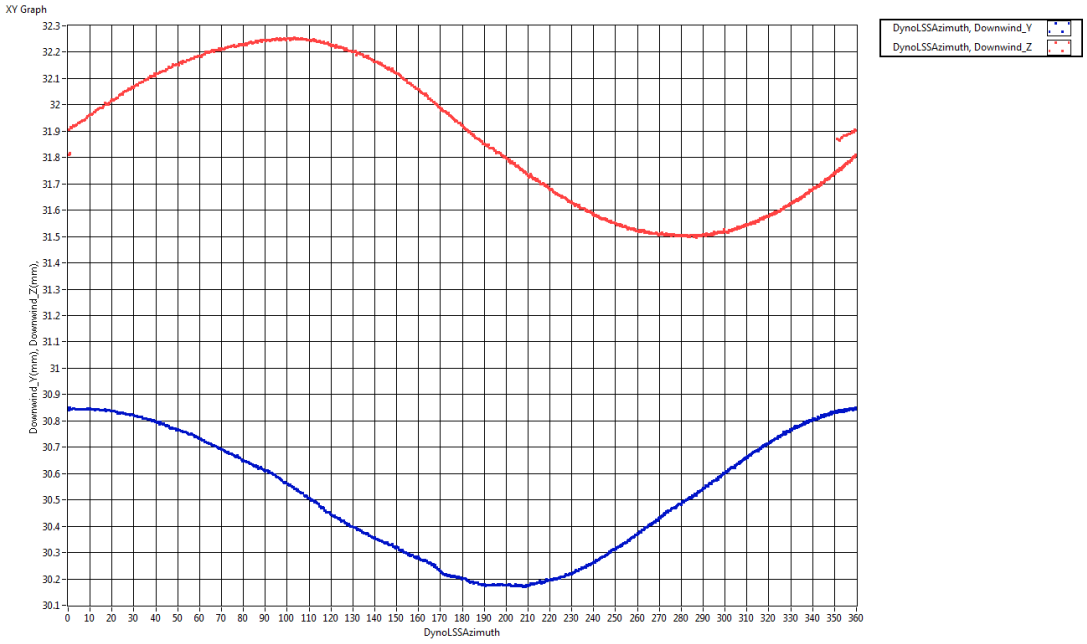

Figure 15. LSS coupling displacement data

3.7 NTL Forces and Displacements

The NTL control system reads the measurements of actuator forces from pressure transducers located on each actuator. It then converts these pressures to forces and moments at any axial position along the main shaft axis. The NTL system uses data from displacement sensors on each actuator to calculate displacements and rotations at any position along the main shaft axis. In the dynamometer, the NTL system and other shaft components exert a large gravity load onto the test drivetrain's main shaft. The NTL actuator loads needed to support this weight are referred to as "tare loads." When applied, the resulting load on the test drivetrain's main shaft should be close to zero. During the setup of the dynamometer, specifically the drivetrain alignment procedure, these tare loads are measured. The NTL controller is then set so that the tare loads are subtracted from the calculated applied loads. Thus, applied loads are commanded and measured based on the loads that are actually applied to the test drivetrain's main shaft flange.

3.8 Test Drivetrain Main Shaft Loads

One method used to determine the tare loads for a given test setup has been to utilize strain gages attached to the LSS of the test specimen. By rotating the shaft slowly and then plotting the stain signals, the amplitude of the oscillation will indicate the shear and bending in the shaft. If the amplitude of the oscillation in this signal can be reduced to zero then the applied loads on the test specimen are zero and the tare has been determined. In practice, this procedure is complicated by the torque required to rotate the shaft at a speed suitable for reading the strain signals and the subsequent overturning moments induced by the flexible couplings.

4 Dynamometer Drive Vibration Characterization

A total of 17 accelerometers were installed across the dynamometer, including the motor, gearbox, NTL device, test stand, and the test drivetrain's gearbox and generator. These locations indicate whether specific speeds or operating conditions are exciting higher-than-normal vibrations. All accelerometers used for this testing were single-axis PCB 352M12 ICP accelerometers. Each sensor was attached to a Micarta block and the blocks were subsequently attached to each component using a two-part epoxy resin.

Figure 65 shows accelerometer positions on the gearbox housing. By using this approach, a baseline of vibration characteristics has been established for comparison against future operating conditions.

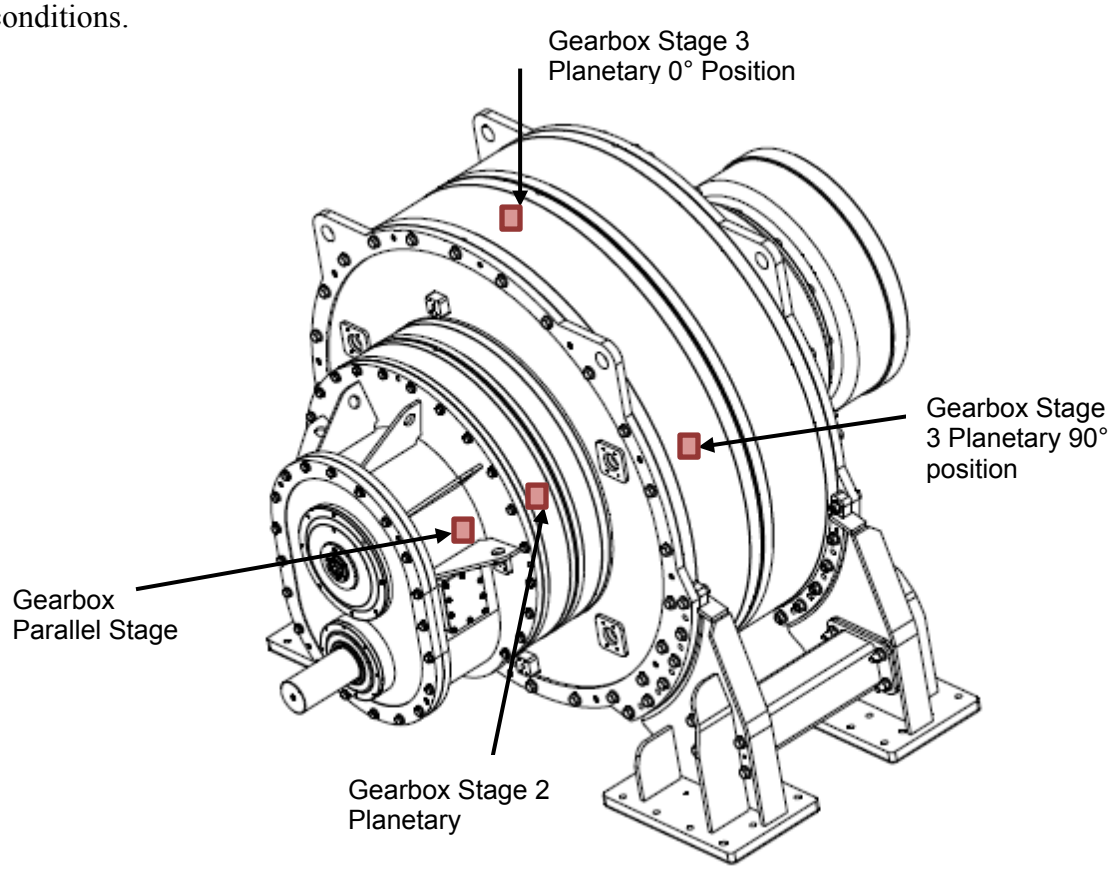

Figure 16. Positions of accelerometers on the gearbox housing. ***Image courtesy of Romax Technology, Inc***

Motor vibrations were captured using two accelerometers: one installed on the drive-end (downwind) bearing and one on the nondrive-end (upwind) bearing. Figure 66 shows the downwind bearing accelerometer placement. The upwind bearing location is identical.

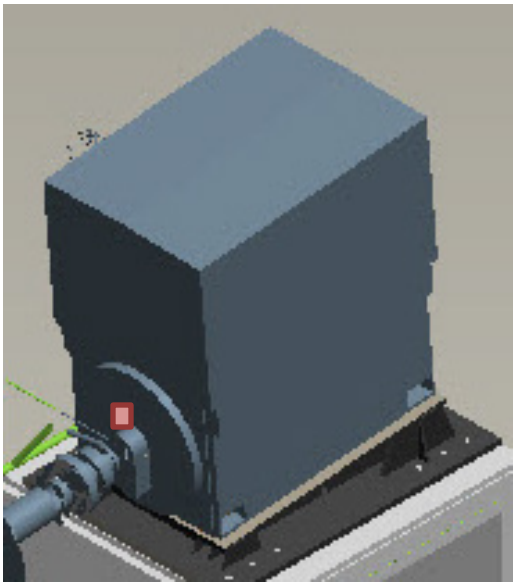

Figure 17. Position of the downwind bearing accelerometer on the dynamometer motor

Three accelerometers were installed on the outer cover, upwind center, and side cover of the NTL device. These locations are illustrated in Figure 67.

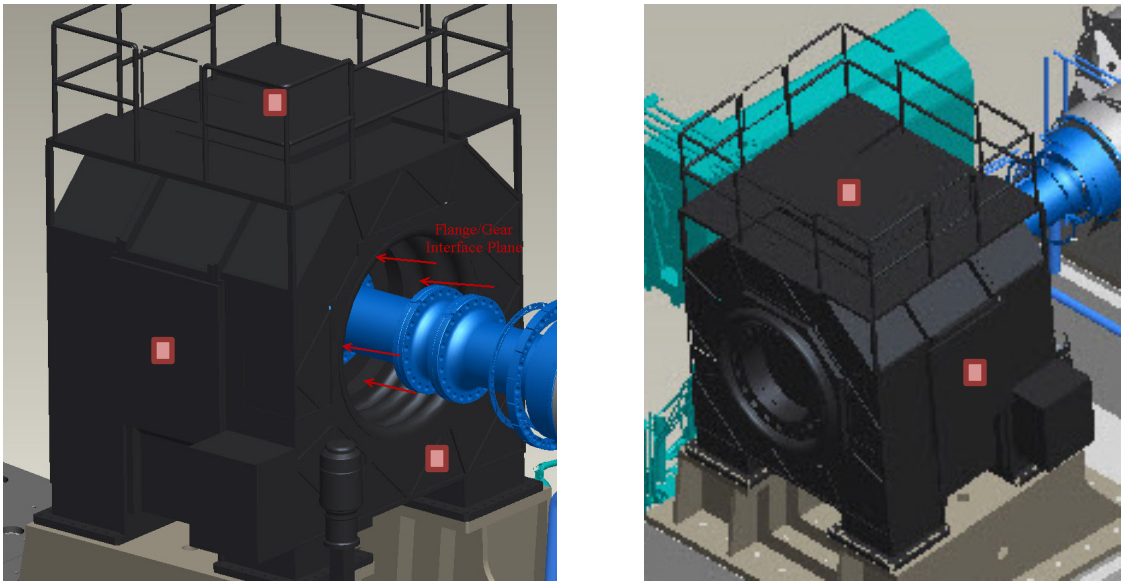

Figure 18. Positions of accelerometers on the NTL device

Six accelerometers were installed on the test drivetrain: two on the LSS bearings, one on top of the downwind bearing, one on top of the gearbox, one on the gearbox trunnion, and one on the generator upwind bearing.

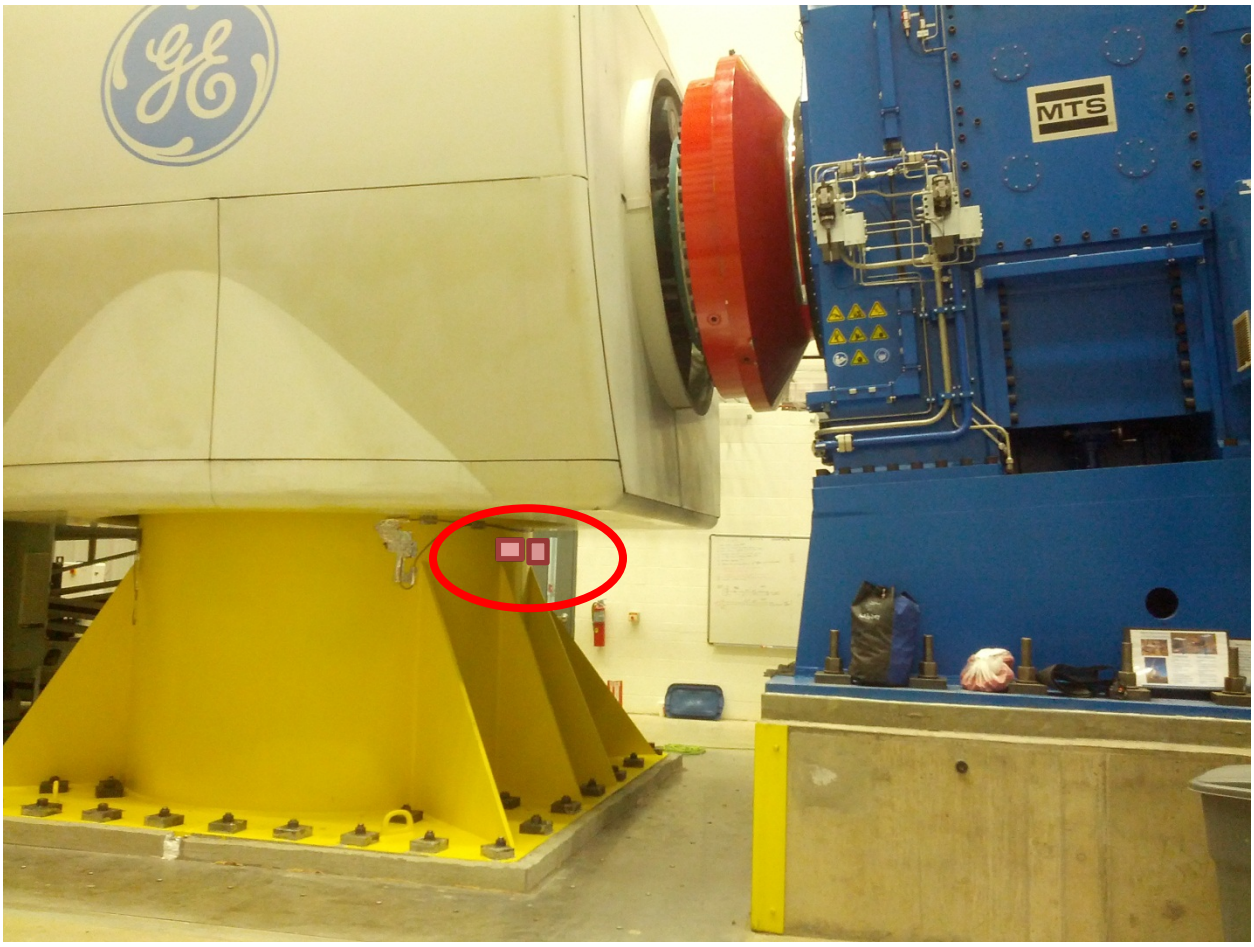

Figure 19. Positions of the accelerometers on the test article test stand. ***Photo by Mark McDade, NREL***

4.1.1 HSS Rotational Speed

The rotational speed of the dynamometer was measured using an retro-reflective sensor. The sensor was installed on the disk brake caliper mounting bracket of the HSS using a magnetic mount. The brake is located downwind of the drive motor. The sensor beam was oriented at the face of the rotor disk and reflective tape was applied to the brake rotor. As the disk rotates, the sensor outputs a single VDC pulse for each rotation, which is used to determine the rotor speed in rpm. The HSS offers finer measurement resolution over the LSS and was chosen to measure rotor speed for this reason.

4.1.2 Data Acquisition System

The system used for this testing was a LMS SCADAS Mobile SCM05 Frontend withV8 ADC Interface Cards. This DAS includes a system controller with an integrated dual tachometer input and Ethernet interface. It was controlled using a test PC with LMS Test.Lab Rev12 software. A project file was created with the appropriate settings to collect vibration data. The LMS hardware and software offer online processing of vibration data with a tracking signal (HSS rpm) to generate acceleration waterfall and spectrogram plots in real time. These features were leveraged for this test.

4.2 Test Sequence

4.2.1 Test Overview

To assess and quantify the vibration characteristics of the dynamometer and probe for unfavorable resonances, it is necessary to conduct an array of test scenarios that represent the broad spectrum of test capabilities. In particular, the dynamometer was tested through a range of speeds with and without torque loads applied. Rotational directionality of the system was also tested by operating the dynamometer rotationally counterclockwise. Finally, a transient event was tested to capture the free-decay response of the drivetrain. The details of these test sequences are further explained in this section.

4.2.2 No-Load Speed Sweeps

The no-load speed sweep tests were conducted with main shaft speeds from zero to 15 rpm to validate speed measurements and as the first check for vibrations or resonance issues. Torque was as required to overcome friction in the drivetrains. The test drivetrain was not connected to the grid and no nontorque loads were applied. The weight of the NTL flange and the GE shaft adapter were sufficient to load the GE main shaft bearings for this test.

The testing procedure was as follows:

1. Arm DAS and acquired data at a sampling rate of 4 kilohertz (kHz)
2. Ramp LSS speed from zero to approximately 15 rpm at a rate of 2 rpm/minute
3. Record data and generate acceleration spectrograms
4. Stop dynamometer rotation and terminate data collection
5. Briefly review vibration spectra to ensure that the data quality is sufficient for further analysis before proceeding.

4.2.3 Loaded Speed Sweeps

After completing the no-load speed sweeps, we executed a series of torque-load speed sweeps. A total of three speed sweeps were conducted with varied torque levels for each sweep. The applied torque levels were 500 kNm, 1,000 kNm, and 1,500 kNm. The data collection and dynamometer operation sequence was the same for each speed sweep.

4.3 Results and Discussion

Due to the large scope of this assessment only a few representative figures will be reviewed and discussed in this report. Spectrograms and waterfall plots, which illustrate vibration amplitude versus frequency and shaft speed are shown in figures 20 thru 22. Spectrogram and waterfall plot data were saved for each test iteration and further analyzed using MATLAB. Specifically, the acquired acceleration spectra were converted to velocity spectra in units of millimeters per second.

4.3.1.1 No-Load Speed Sweep Results

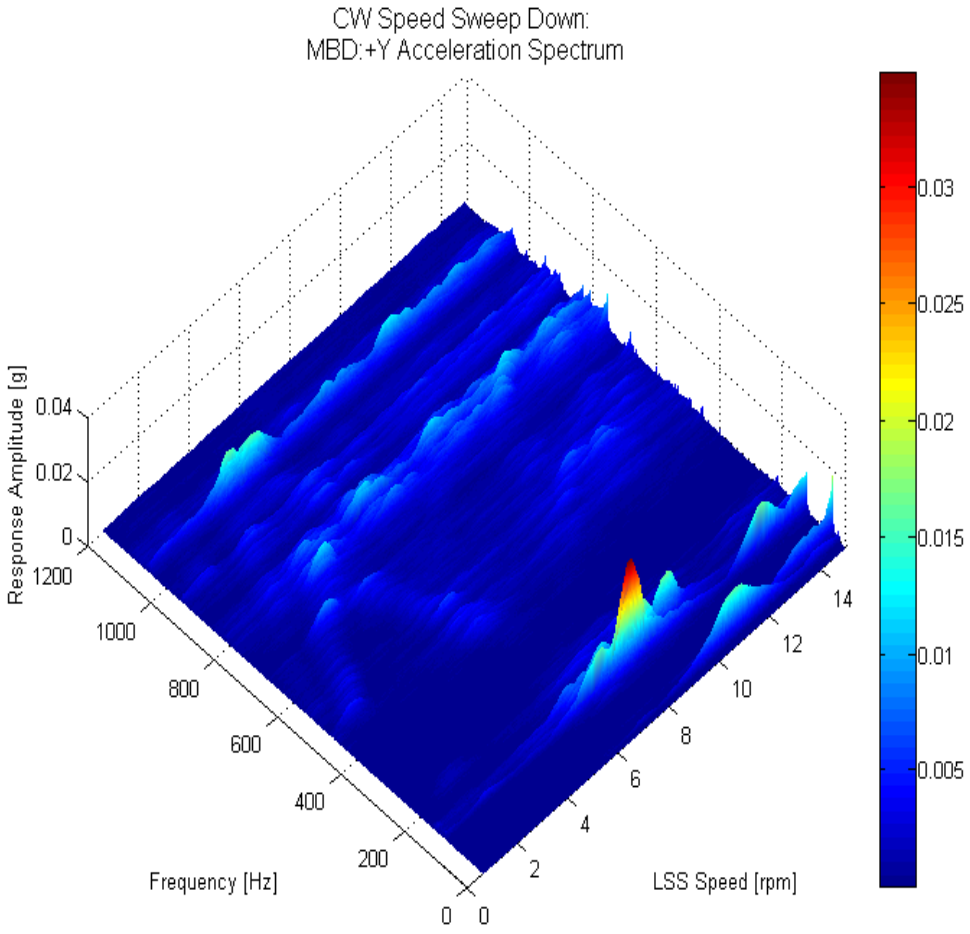

Figure 20. The 5-MW dynamometer downwind motor bearing acceleration waterfall plot

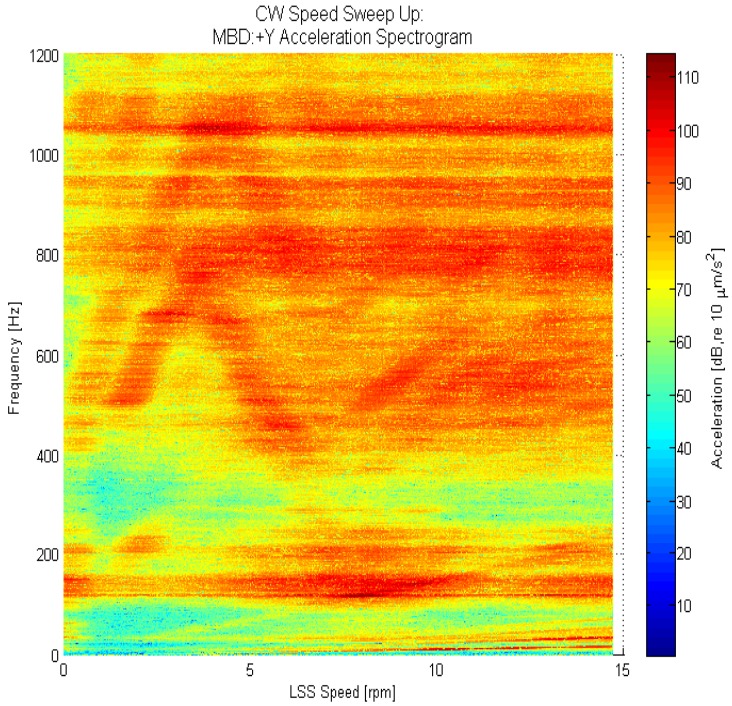

Figure 21. The 5-MW dynamometer downwind motor bearing acceleration spectrogram in decibel (dB) scale

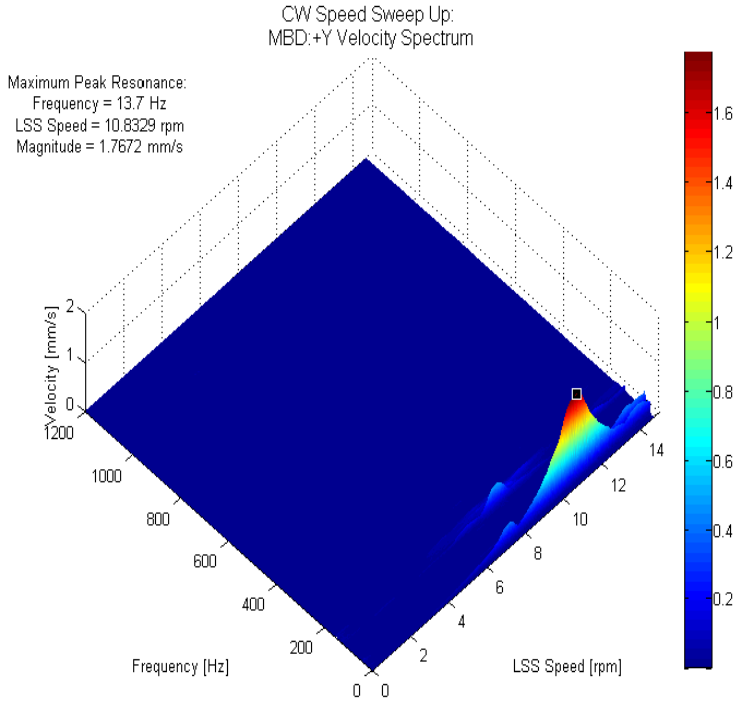

Figure 22. 5-MW dynamometer downwind motor bearing velocity (mm/s) waterfall plot

Table 3. Vibration Testing Signal List

Channel Number	Signal Name	Orientation	Location	Make/Type	Serial Number	Sensitivity	Mainframe Slot	Module Type
1	Tacho	NA	HSS Brake Disk	IFM Electronic OGP503	NA	NA	04	Integrated
2	MBU	Z	Motor Bearing Upwind	PBC 352M12	322	1,017 millivolt per g(mV/g)	01	V8
3	MBD	Z	Motor Bearing Downwind	PBC 352M12	517	969 mV/g	01	
4	GBPS	Y	Gearbox Parallel Stage	PBC 352M12	349	950 mV/g	01	
5	GBS2P	Z	Gearbox Stage 2 Planetary	PBC 352M12	2041	928 mV/g	01	
6	GBS3P90	Y	Gearbox Stage 3 Planetary 90° position	PBC 352M12	9480	949 mV/g	01	
7	GBS3P0	Z	Gearbox Stage 3 Planetary 0° Position	PBC 352M12	342	964 mV/g	01	
8	NTLTC	Z	NTL Top Cover	PBC 352M12	335	982 mV/g	01	
9	NTLCC	Z	NTL Center Cover	PBC 352M12	528	961 mV/g	01	
10	NTLSC	Y	NTL Side Cover	PBC 352M12	350	949 mV/g	02	
11	TALSSUB	Z	Test Article LSS Upwind Bearing	PBC 352M12	530	982 mV/g	02	
12	TALSSDB	Z	Test Article LSS Downwind Bearing	PBC 352M12	8187	967 mV/g	02	
13	TAGBT	Z	Test Article Gearbox Top	PBC 352M12	2038	978 mV/g	02	
14	TADB	Z	Test Article Downwind Bearing	PCB 352M12	344	993 mV/g	02	
15	TAGBTrun	Z	Test Article Gearbox Trunnion	PBC 352M12	2032	943 mV/g	02	
16	TAGUB	Z	Test Article Generator Upwind Bearing	PCB 352M12	323	973 mV/g	02	
17	TSU-X	X	Test Stand Upwind	PBC 352M12	2042	978 mV/g	02	
18	TSU-Y	Y	Test Stand Upwind	PBC 352M12	1120	1,020 mV/g	03	

5 CGI Characterization Testing

5.1 CGI Technical Characteristics

The CGI's electrical topology is based on ABB's ACS6000 variable-speed-drive power converter blocks that are combined into the system as shown in Figure 23. On a test article side, four ACS6000 active inverters are combined in parallel to provide sufficient short-circuit-current capability. These inverter units are labeled as INU 1-4 in Figure 23. High short-circuit-current capability is an important feature when testing wind turbine generators that have their stator windings directly coupled with the power grid (Types 1, 2, and 3 wind turbines). The inverters are connected to the custom-made 7-MVA power transformer with six windings that are combined in parallel and series manner on the low- and high-voltage sides, respectively. This unique transformer configuration allows for four-wire operation (three phases and neutral) and independent control of each phase voltage. This way, any desired voltage fault scenario (under and overvoltage, symmetrical or nonsymmetrical) can be achieved.

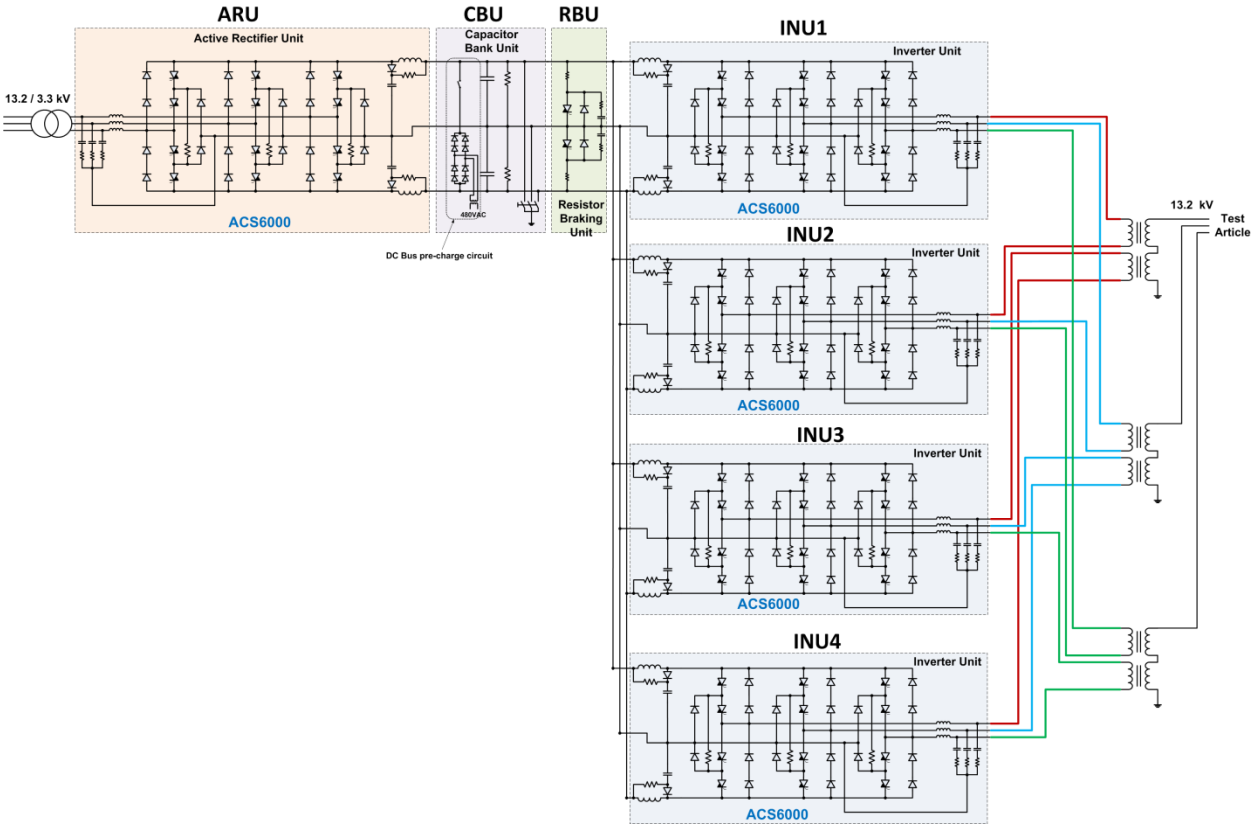

Figure 23. CGI electrical topology

On the line side, the CGI consists of a single ACS6000 active rectifier module that is labeled as active rectifier unit (ARU) in Figure 23. The ARU is connected to the NWTC power grid via a conventional pad mount step-up transformer. Both the test and line-side voltages are decoupled via a DC link that consists of a capacitor bank unit (CBU) with pre-charging and grounding circuits as shown in Figure 23. There is also a resistive braking unit (RBU) that is designed to protect the DC bus from overvoltage conditions.

The CGI has two types of controls that operate independently from each over: the inverter unit (INU) master controller uses an ABB AC800PEC real-time controller that is responsible for INU operation based on set points from NREL's supervisory control and data acquisition (SCADA) system, and for INU and transformer protection. The ARU control is based on a standard ASC6000 topology, and is independent of the INU's control. The architecture of the CGI's ARU and INU controls is shown in Figure 24. The main components of the control system include the:

- Application and motor controller (AMC). A digital signal processor for the ACS600 control system.
- Power plate (PUB). The communication system unit for branching.
- Interface boards (INT) for the ARU and INU modules
- Real-time power electronics controller (RT PEC)

A special modulation algorithm is implemented in the INU control to ensure the low-voltage total harmonic distortion (THD) and adequate dynamic response needed for the grid simulator application.

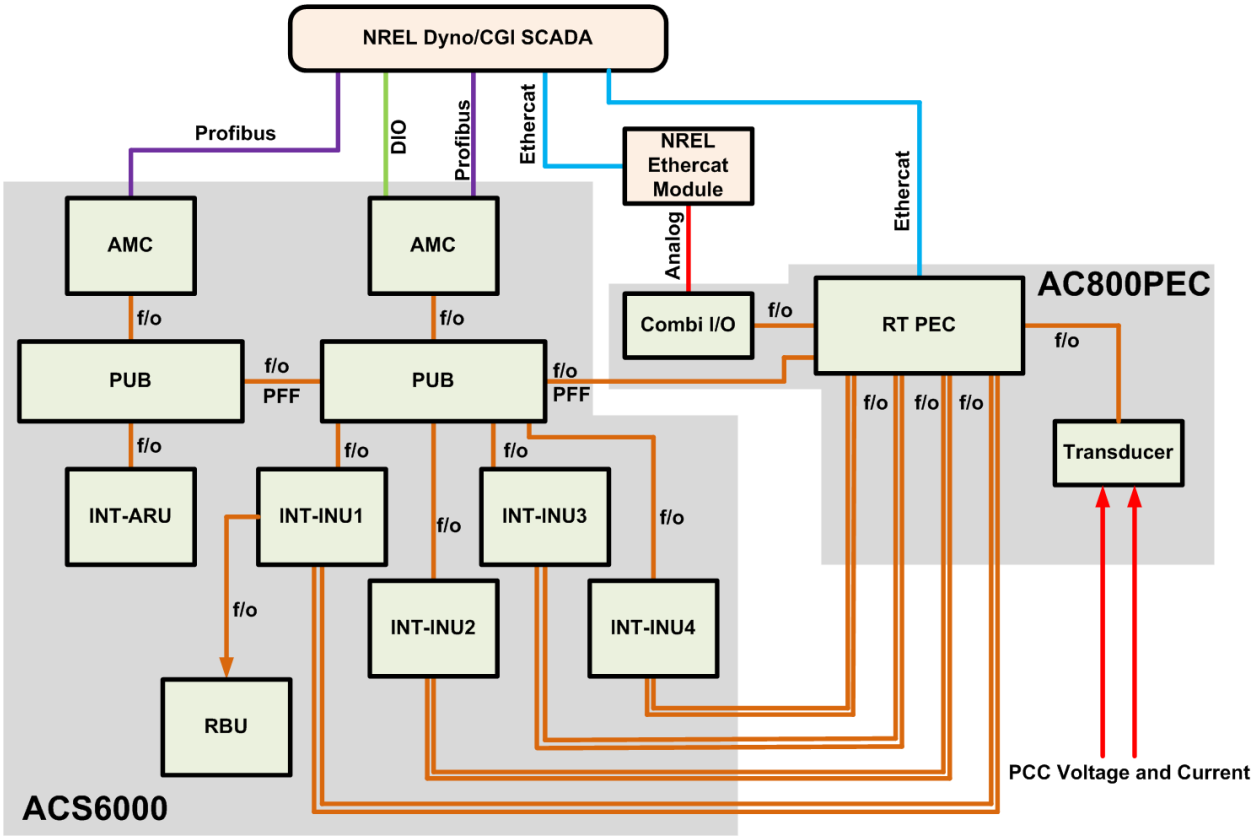

Figure 24. The CGI controls architecture

The commanded voltage amplitudes, phase angles, and frequency are communicated from the NREL SCADA interface using the Ethernet for Control Automation Technology (EtherCAT) communication protocol and hardware. Safe start-up and shut-down controls based on magnetizing characteristics of the CGI transformer are also implemented in the NREL SCADA

system. Additional control parameters, such as maximum rate of change of voltage, voltage droop compensation, and reference values, are set by NREL SCADA. The safety of the CGI's operation is ensured by the system of software watchdogs and hard-wired protection schemes that also incorporate protection of the test article. Other protection schemes (such as the CGI transformer anti-saturation control, over current protection, and so on) are implemented in the AC800PEC controller.

The CGI's main technical characteristics are shown in Figure 25. The CGI produces voltages at the 13.2-kiloVolt (kV) level. It is capable of continuous operation under 7-MVA load levels and voltage fault testing for any types of existing wind turbine generator topologies. The CGI is also suited for testing other types of inverter-coupled generation, such as photovoltaic, energy storage, and fuel cells. Conventional synchronous generation (e.g., diesel generators, small gas turbines, and so on) can be easily tested with the CGI as well.

CGI high-voltage fault testing can be performed if the transformer winding is set at a higher tap position. Over 130% overvoltage conditions can be created on CGI terminals if operating this mode. This transformer tap position is manually set by the NREL operator (transformer must be de-energized for this).

Other CGI characteristics include such unique features as the possibility to create long-term voltage abnormalities like amplitude oscillations, sub-synchronous resonance conditions, and programmable distortions. Also, the CGI is capable of simulating both 50- and 60-Hz grids continuously as well as creating all types of frequency excursions that might exist in different types of power systems (e.g., large interconnected power systems, islands, and microgrids). This feature is especially important for testing the frequency response characteristics of wind turbine and other renewable technologies.

5.2 CGI Commissioning Configuration

The CGI was commissioned using the 2.75-MW wind turbine generator drivetrain installed in NREL's 5-MW dynamometer facility. The diagram in Figure 25 shows the interconnection between the CGI and test article. Electrically, the wind turbine under test consists of a permanent-magnet synchronous generator with the system of five 690-volts alternating current (VAC) power electronic converters in parallel. The turbine transformer steps the voltage to 13.2 kV, so it can be connected to the CGI's terminals via a system of underground megavolt cables and switchgear. The turbine transformer windings are protected from overvoltages by a system of metal-oxide varistors which are installed in the switchgear.

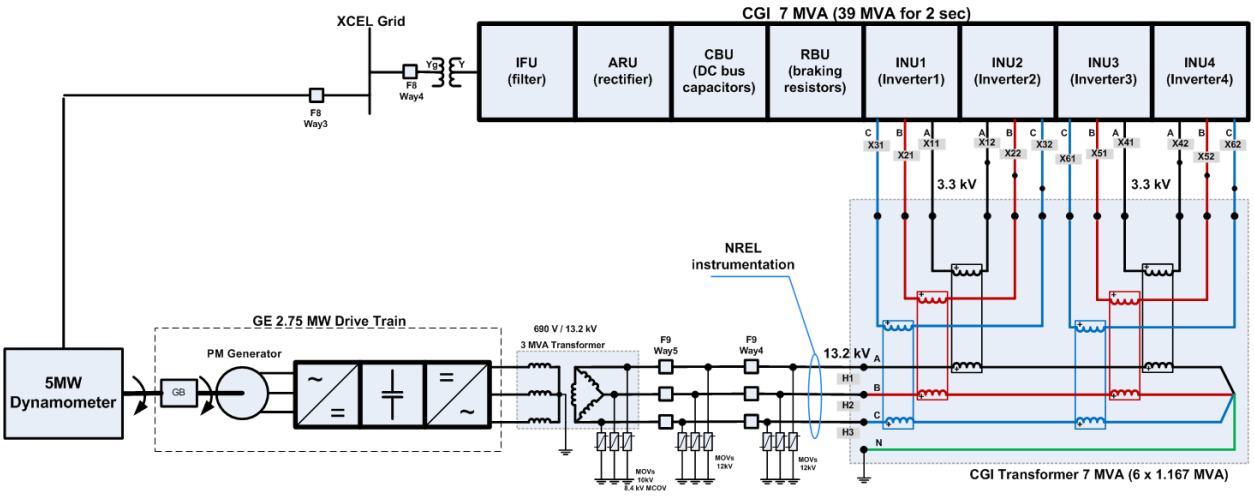

Figure 25. Test configuration

The 13.2-kV side of the turbine transformer winding is configured as a Δ delta connection, so there is no neutral wire connected coming out of the test article. For this reason, the neutral terminal of the CGI transformer is grounded as shown in Figure 25.

NREL has built a custom high-bandwidth /high-accuracy instrumentation system to monitor and analyze the CGI's voltage and current waveforms. Its voltage measurements are based on CIC precision high-voltage differential probes (model DP20-10K). These voltage probes are rated for 20-kV peak-to-peak voltages with up to a 100-megahertz frequency bandwidth. CGI current measurements are based on Powertek RCTi 1.3 kiloAmpere flexible Rogowski probes. The connection diagram of the CGI MV instrumentation is shown in Figure 26. National Instruments cDAQ-9172 chassis with NI 9229 24-bit analog input models are used to sample the three-phase voltage and current waveforms from the MV instrumentation. These waveforms are sampled at a 50-kHz sampling frequency for all channels. An NREL-developed custom-made Labview interface is used to process, analyze, visualize, and record the high-speed data collected from the CGI instrumentation. An example control window of the NREL interface is shown in Figure 27. Active and reactive powers, power factors, electrical frequencies, RMS voltages and current, harmonics and distortions are calculated by NREL Labview system from voltage and current waveforms.

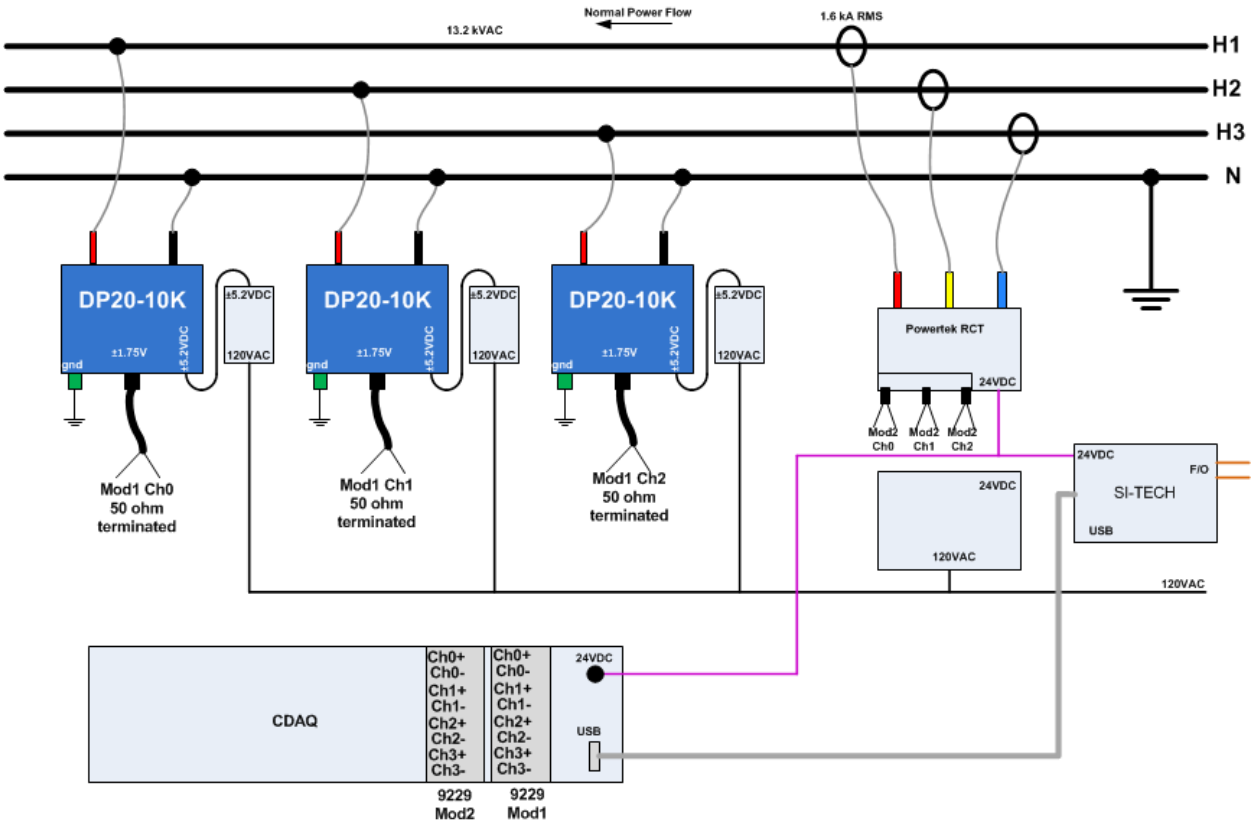

Figure 26. Diagram of NREL MV instrumentation

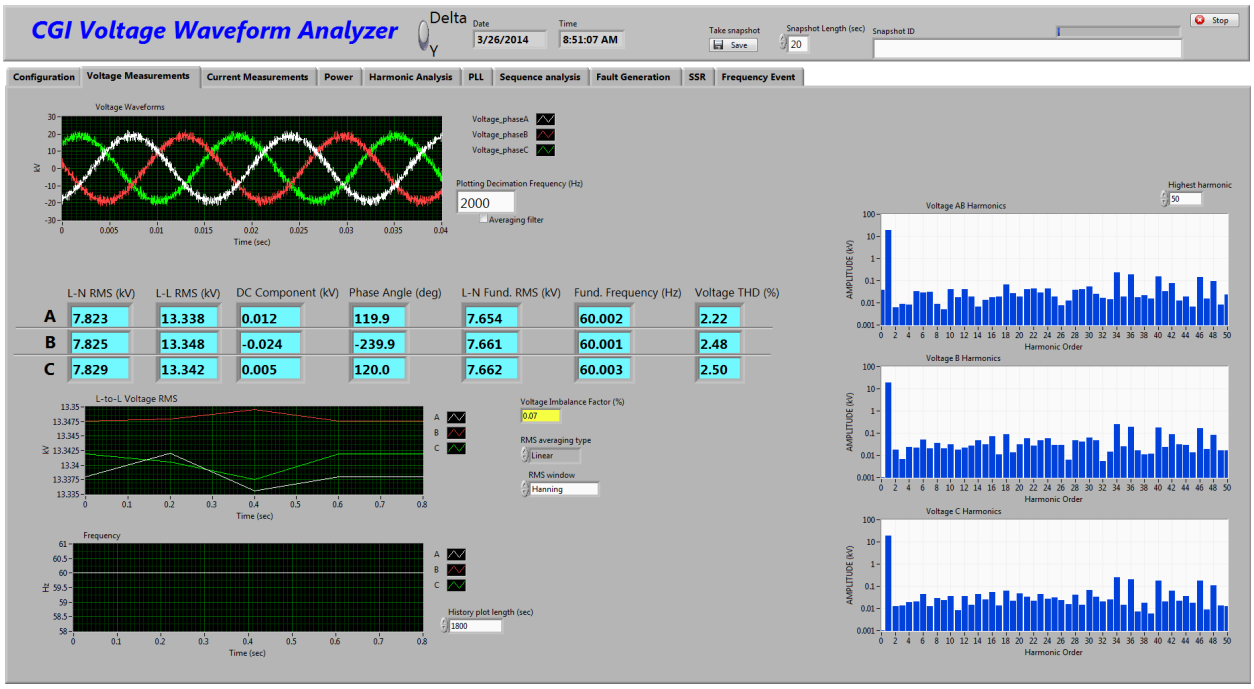

Figure 27. Interface of the NREL-developed Labview system for CGI testing

5.3 CGI Characterization Testing

5.3.1 Test Matrix

We performed CGI commissioning and characterization testing in accordance with the test matrix shown in Table 4 under different load conditions using the GE 2.75-MW wind turbine generator. During testing activities, the CGI demonstrated stable operation and fully met (and in some cases excelled) all design requirements and specifications. It is difficult to show all of the CGI test results in one document because of space limitations. In this report we show the most important results that demonstrate the unique features of the CGI in the area of grid integration testing for wind power technologies.

Table 4. CGI Characterization Test Matrix

	Turbine Load					
Test Type	**No Load**	**20% (550 kilowatts [kW])**	**40% (1.1 MW)**	**60% (1.65 MW)**	**80% (2.2 MW)**	**100% (2.75 MW)**
Software protection testing	✓					✓
CB protection testing	✓					✓
One-phase voltage drops*	✓	✓	✓	✓	✓	✓
Two-phase voltage drops*	✓	✓	✓	✓	✓	✓
Three-phase voltage drops*	✓	✓	✓	✓	✓	✓
One-phase overvoltage **	✓	✓	✓	✓	✓	✓
Two-phase overvoltage **	✓	✓	✓	✓	✓	✓
Two-phase overvoltage **	✓	✓	✓	✓	✓	✓
Voltage phase jump tests (±10°, ±30°)	✓					✓
Voltage amplitude variations	✓					
Frequency variations	✓					✓
Grid impedance variations (10% resistive, inductive, and capacitive)						✓
Transformer impedance compensation tests						✓
Steady-state 50-Hz tests	✓					
Parallel operation of two dynamometers						✓

* Voltage drop tests were conducted for 20, 40, 60, 80, and 100% low voltages with fast and slow recovery with the transformer in tap position 1
** Overvoltage tests were conducted for 10%, 20%, and 30% overvoltage conditions with fast and slow recovery with the transformer in tap position 2

5.3.2 No-Load Voltage Waveform Characterization

Characteristics of no-load voltage waveforms are important because they determine the quality of the MV waveform produced by the CGI. Characteristics of no-load voltage waveforms are important for two reasons:

- High-voltage distortions can cause the test equipment to malfunction and the transformer to overheat and create conditions for harmonic resonances
- Excessive voltage distortions can become a problem for synchronizing a test article with the CGI.

For these reasons, it was required during the design stage for the CGI no-load voltage THD not to exceed 5% and with no significant contribution from lower harmonics.

The measured voltage waveforms on the CGI's MV terminal are shown in Figure 28 and Figure 29 for line-to-neutral and line-to-line cases, respectively. The FFT spectrum of the line-to-line voltage waveform is shown Figure 30 with logarithmic scales on both the X- and Y-axis. The harmonic spectrum of the same voltage is shown in Figure 31 for up to the 50th harmonic component of the 60-Hz fundamental component. The THD of the steady-state line-to-line voltage does not exceed 3.4%, with little contribution from lower harmonic components.

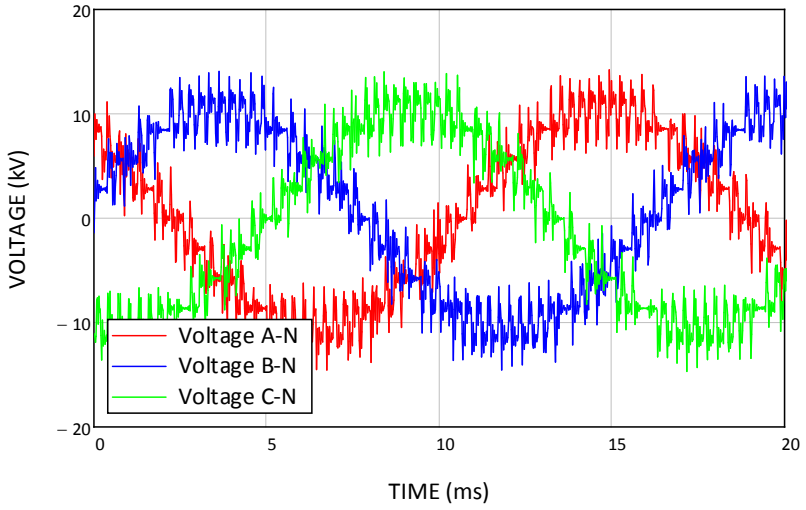

Figure 28. The CGI no-load voltage waveforms (line-to-neutral)

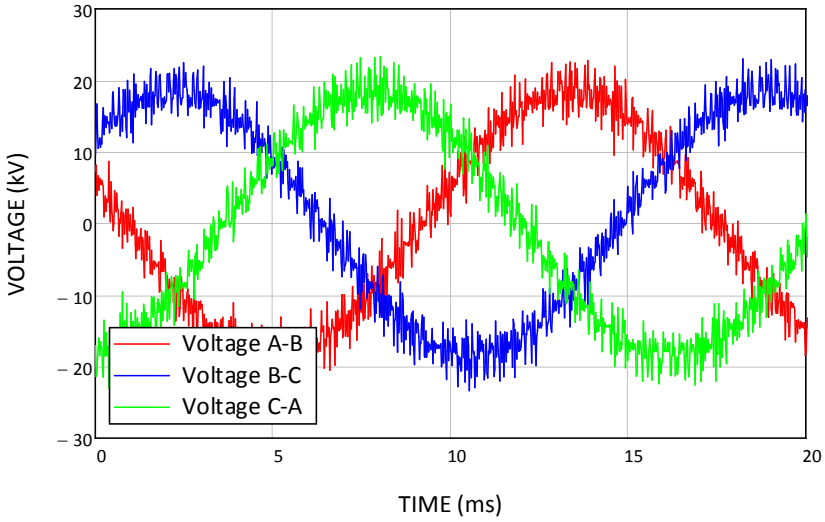

Figure 29. The CGI no-load voltage waveforms (line-to-line)

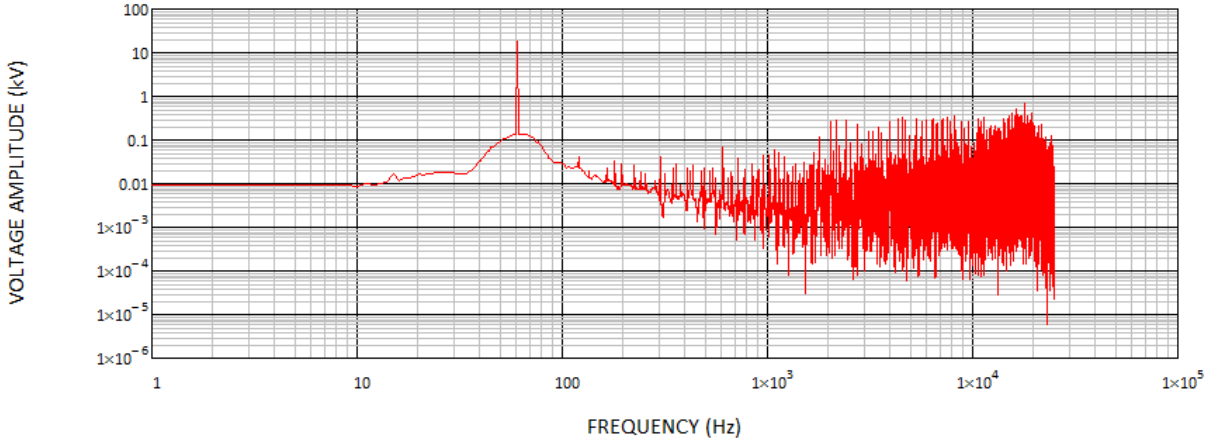

Figure 30. FFT spectrum of the no-load line-to-line voltage

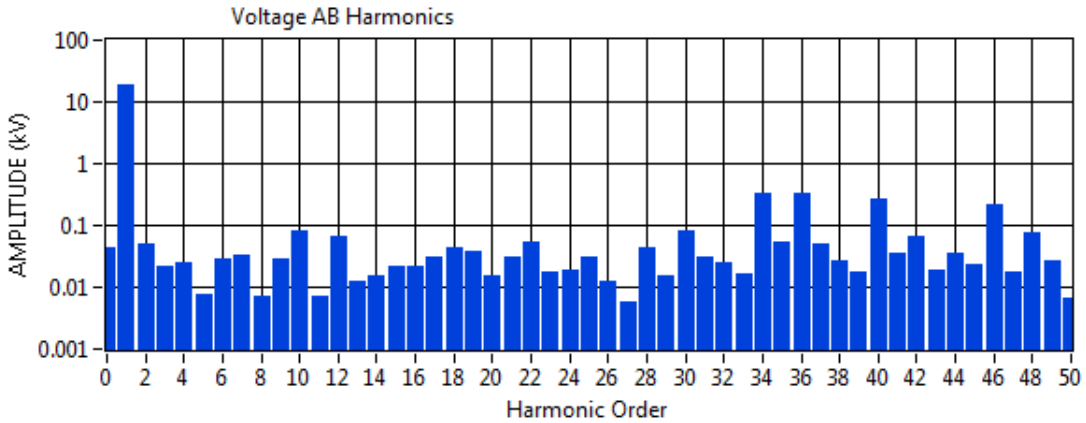

Figure 31. No-load line-to-line voltage harmonics (THD = 3.35%)

5.3.3 Voltage Waveforms Under Turbine Load

Voltage waveforms on the CGI MV terminals when operating at the full load of the 2.75-MW wind turbine are shown in Figure 32 and Figure 33 for the line-to-neutral and line-to-line measurements, respectively. The FFT spectrum of the line-to-line voltage waveform under full load is shown in Figure 34, and the harmonic spectrum of the same voltage is shown in Figure 35. The THD of the steady-state line-to-line voltage is below 2.4%. The line current waveforms measured on the CGI's MV terminals are shown in Figure 36.

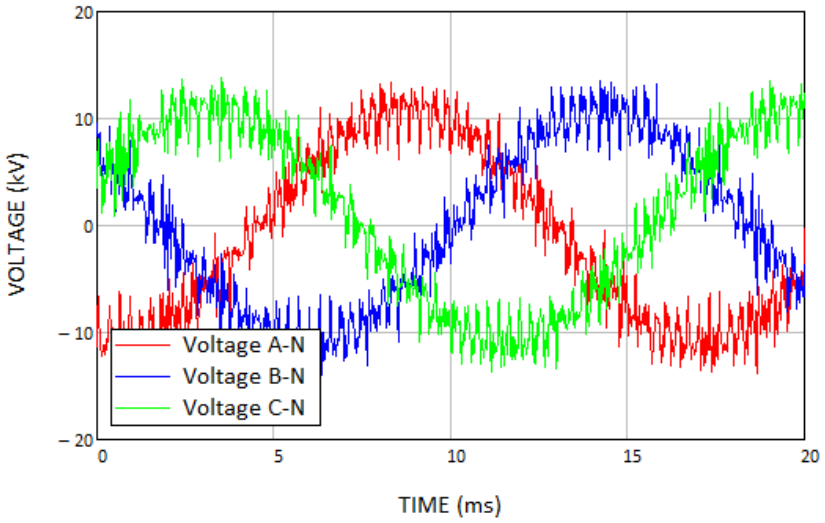

Figure 32. The CGI line-to-neutral voltage waveforms under the 2.75-MW load

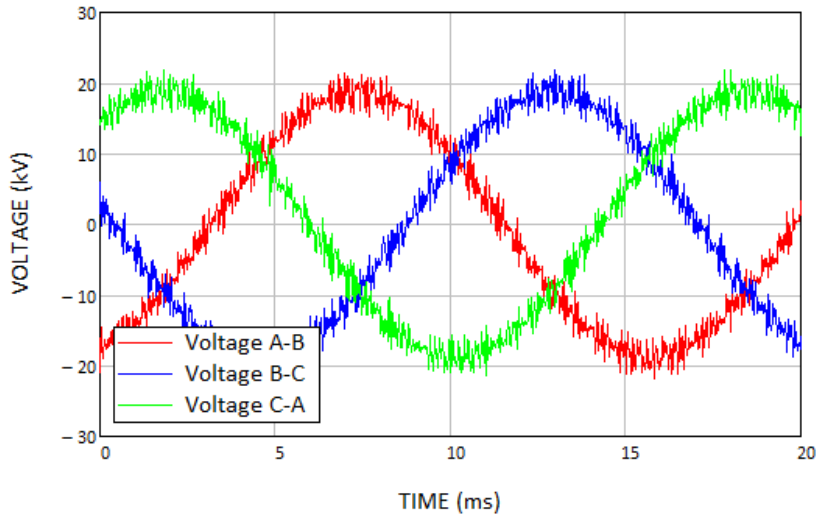

Figure 33. The CGI line-to-line voltage waveforms under the 2.75-MW load

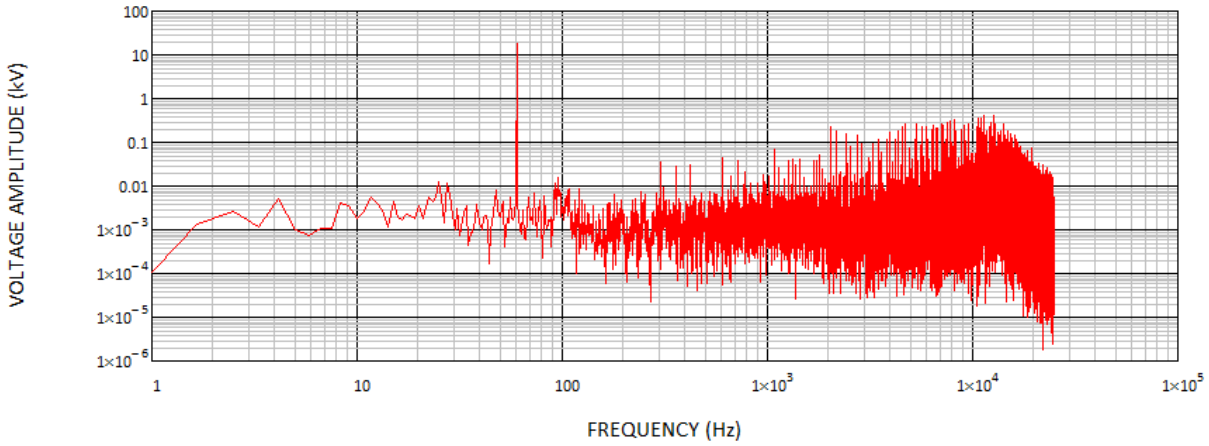

Figure 34. Spectrum of the line-to-line voltage under the 2.75-MW load

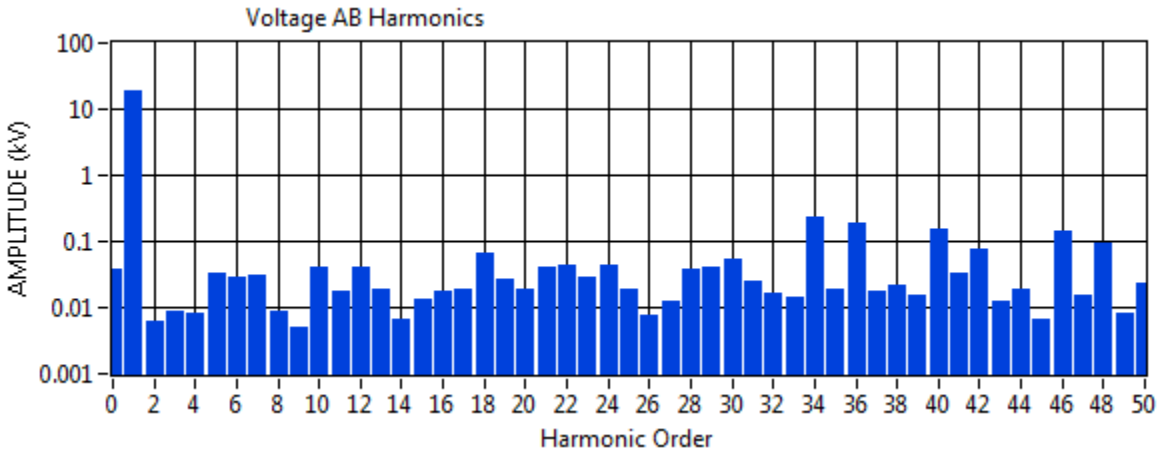

Figure 35. Line-to-line voltage harmonics under the 2.75-MW load (THD = 2.4%)

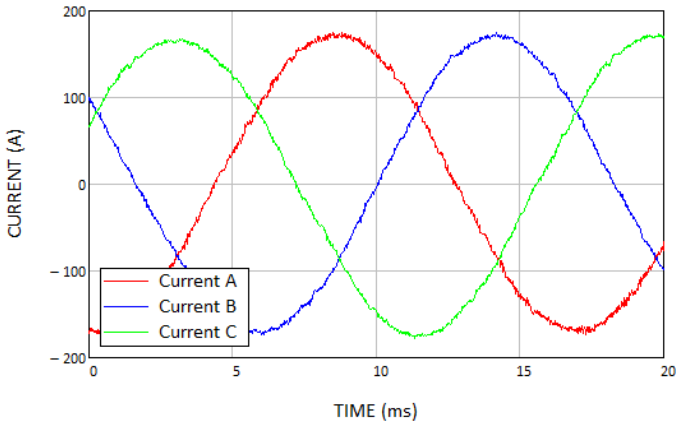

Figure 36. The CGI current waveforms under the 2.75-MW load

5.3.3.1 Single-phase 100% voltage drop tests under the full turbine load

As indicated in Table 4, we conducted a series of low-voltage tests on the GE 2.75-MW wind turbine generator at different load levels. The 100% drop (or zero voltage) cases are the most challenging ones in terms of the CGI's and wind turbine's operations. In this section, we show results for the single, two-, and three-phase voltage drop tests when the 2.75-MW GE turbine was operating at its rated generation level. The CGI terminal voltages were commanded from their nominal 13.2-KV values to zero level. Two recovery cases were emulated for all fault conditions: the fast-recovery case, when the CGI voltages were commanded back to their nominal prefault value in 100 millisecond intervals, and the slow-recovery case, when voltages were commanded to restore their nominal prefault level with slow 2- or 3-s ramping. The resulting graphs for single, two-, and three-phase 100% voltage drops for both fast and slow-recovery conditions are consolidated in Figure 37 to Figure 42. As shown in these figures, the CGI acts as a stable voltage source for all symmetrical and nonsymmetrical conditions despite wind turbine behavior. The wind turbine introduces oscillatory dynamics in both active and reactive power especially for nonsymmetrical cases (single- and two-phase faults). The CGI is capable of accurately controlling its terminal voltage in accordance with NREL SCADA set points regardless of large swings in turbine active and reactive power.

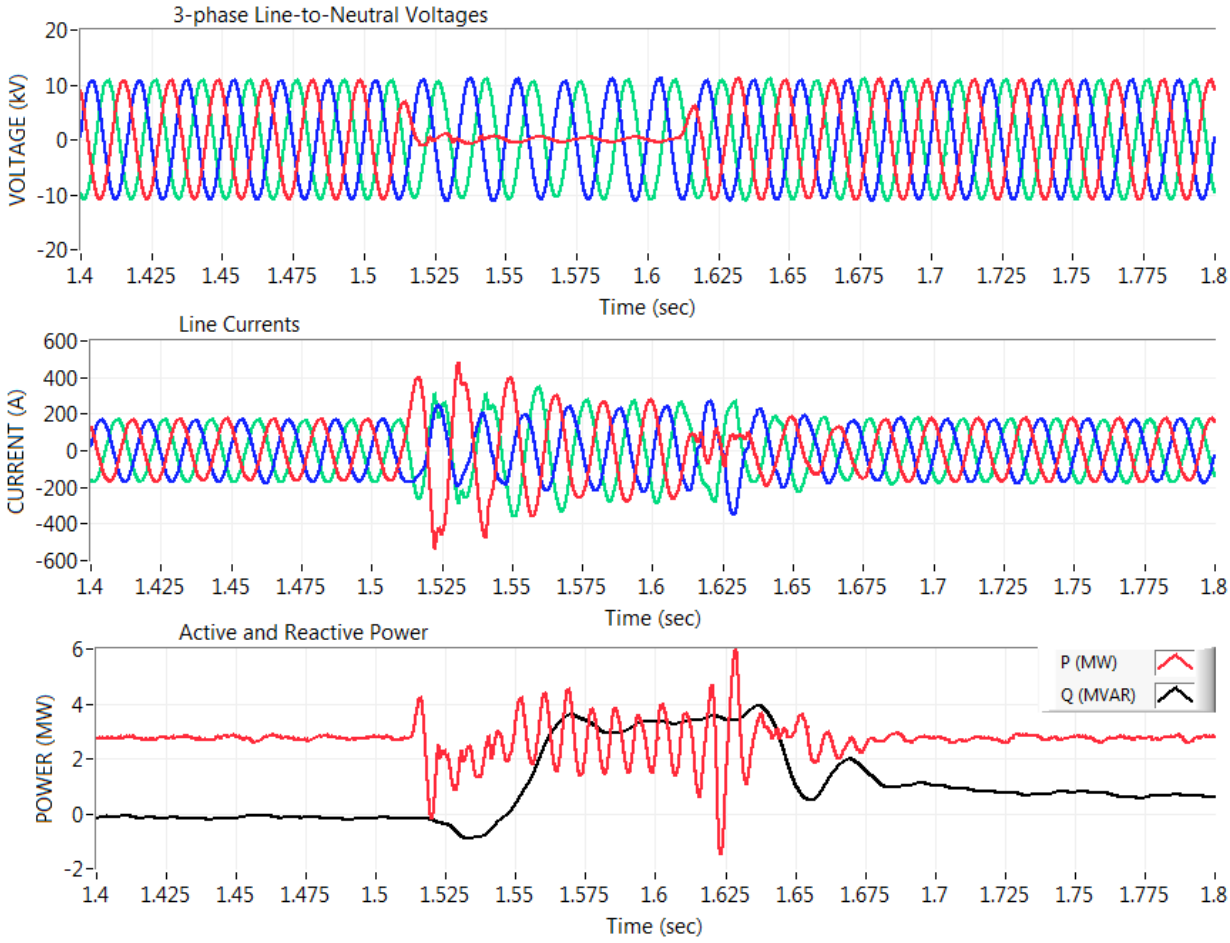

Figure 37. A single-phase voltage fault with fast recovery

The power converters of the GE turbine are equipped with chopper resistors with 3 MW of combined power. The large swings in turbine power above its rated level are absorbed by these resistors to protect the converter DC bus from overvoltages.

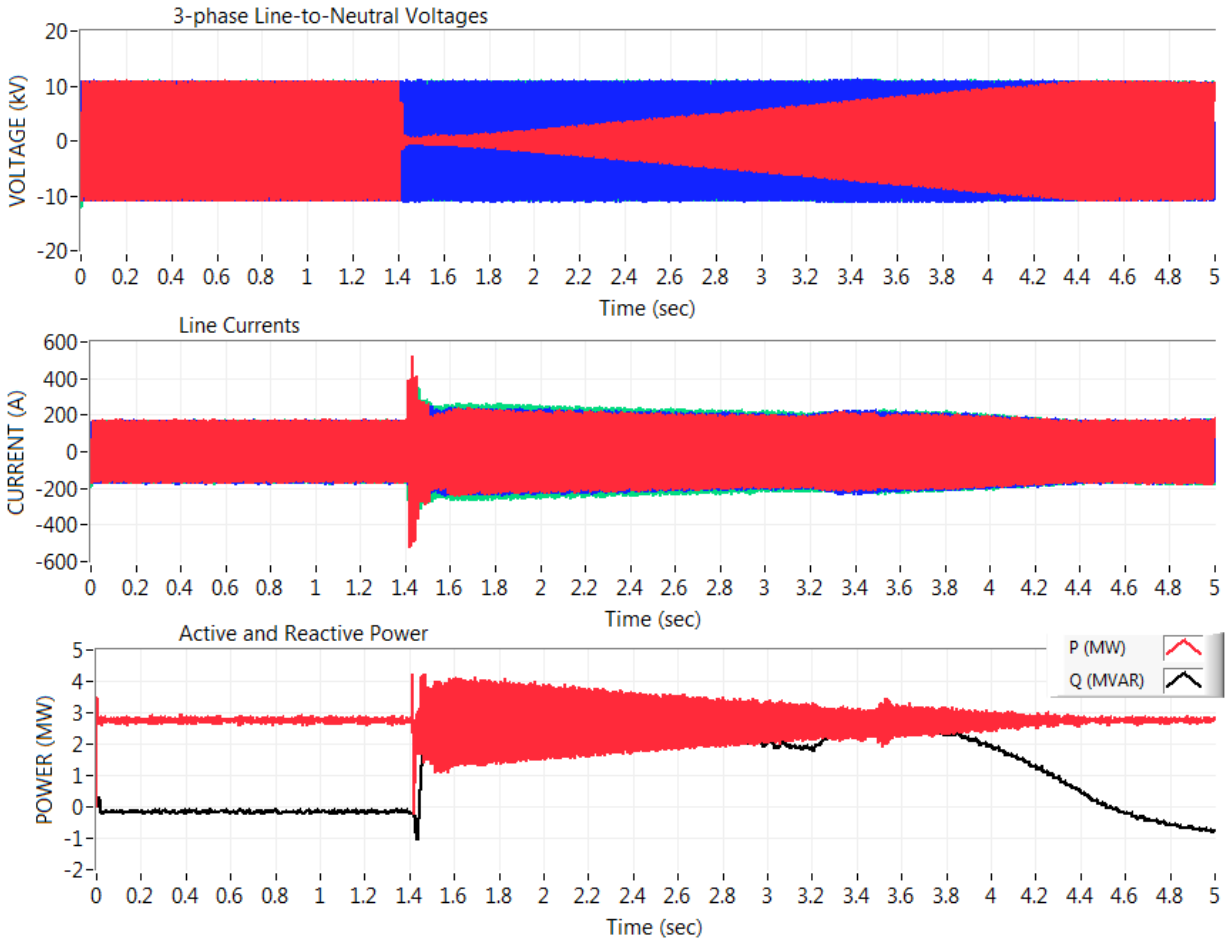

Figure 38. A single-phase voltage fault with a slow 3-s recovery

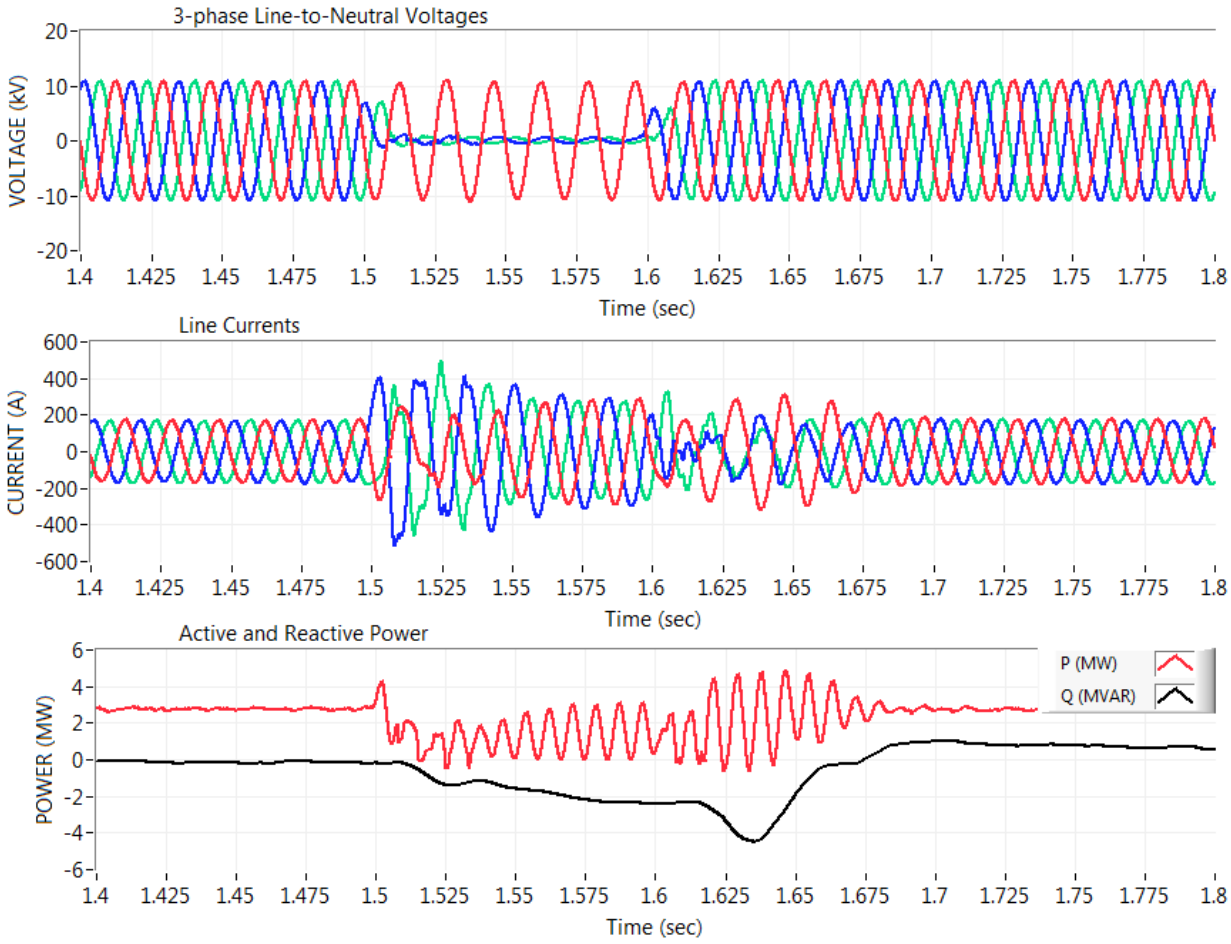

Figure 39. A two-phase voltage fault with fast recovery

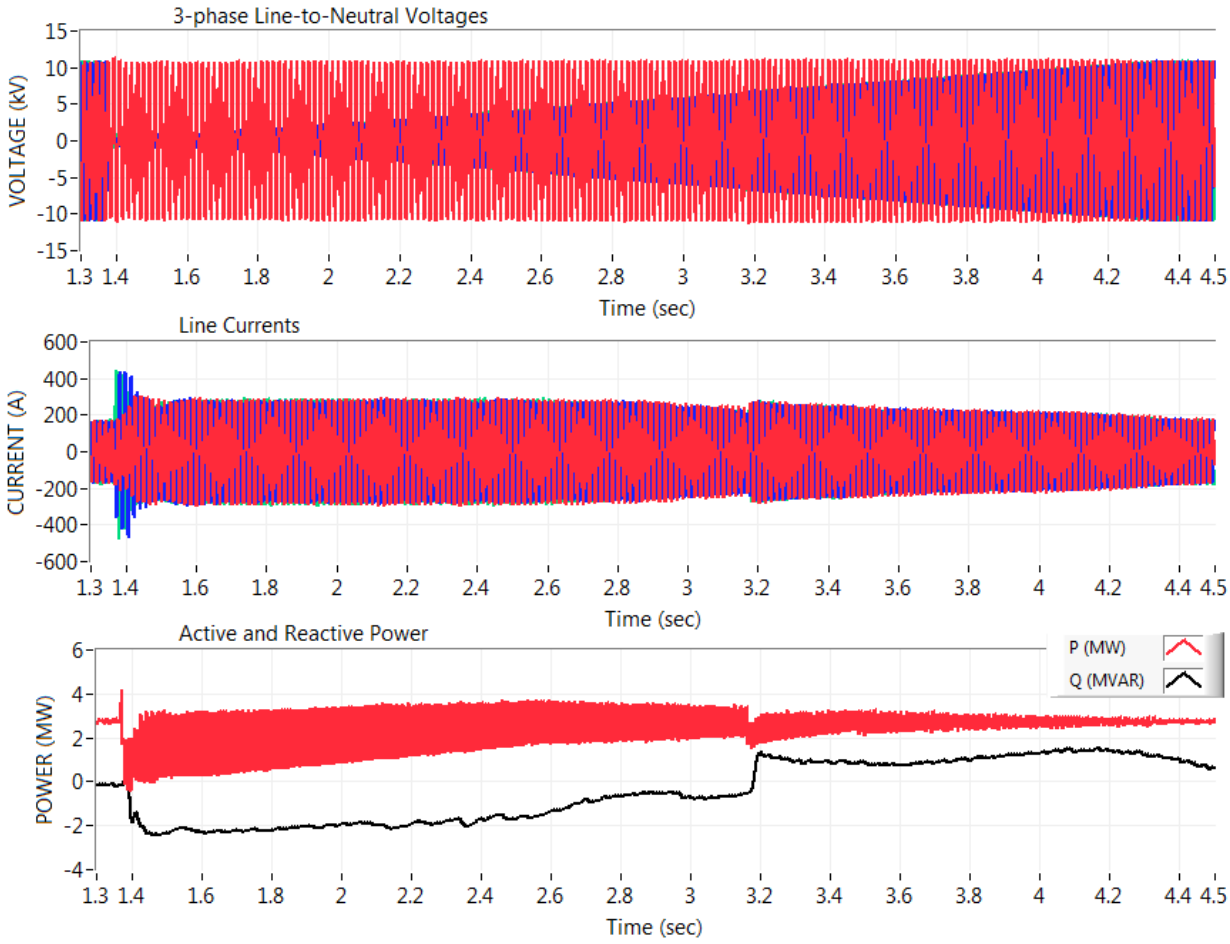

Figure 40. A two-phase voltage fault with slow recovery

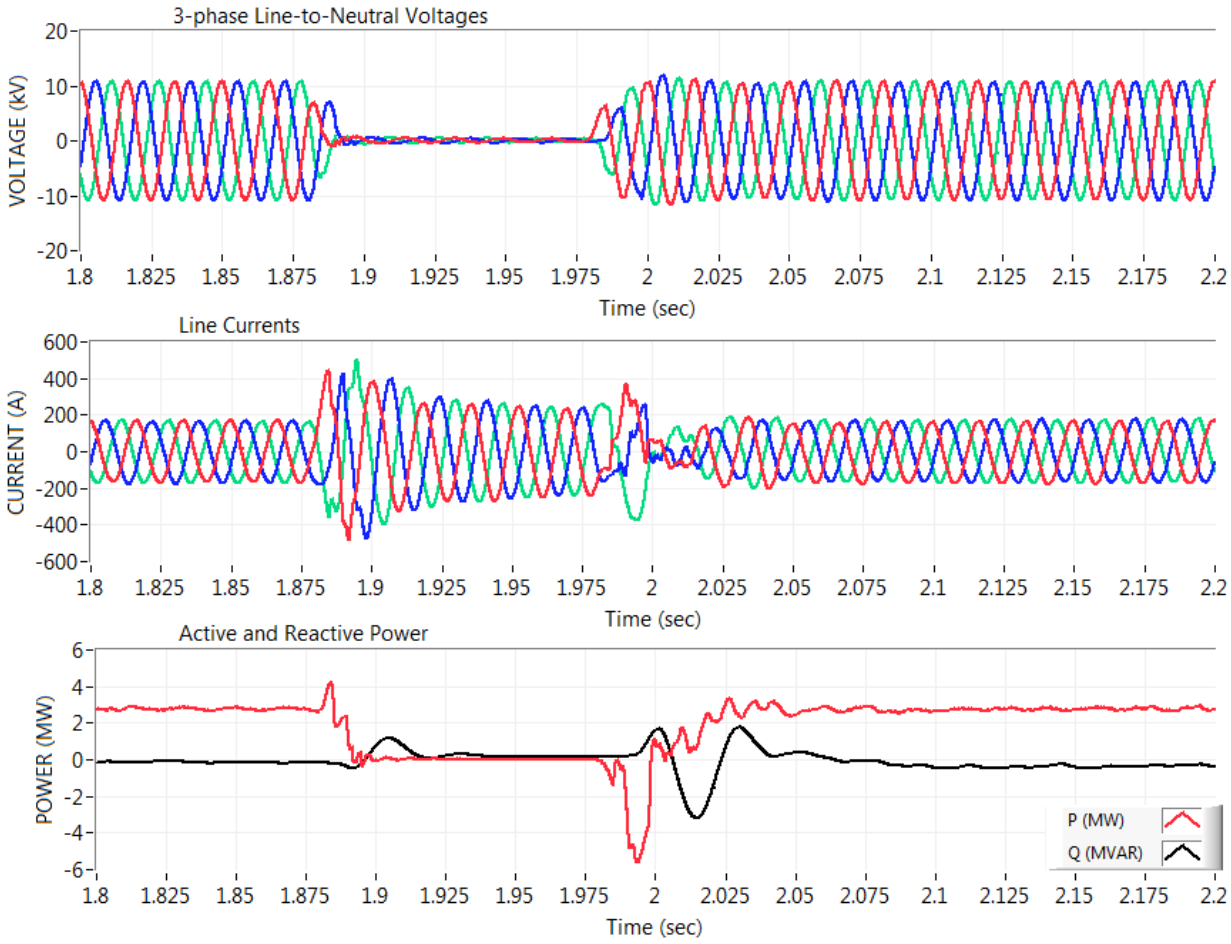

Figure 41. A three-phase voltage drop with fast recovery

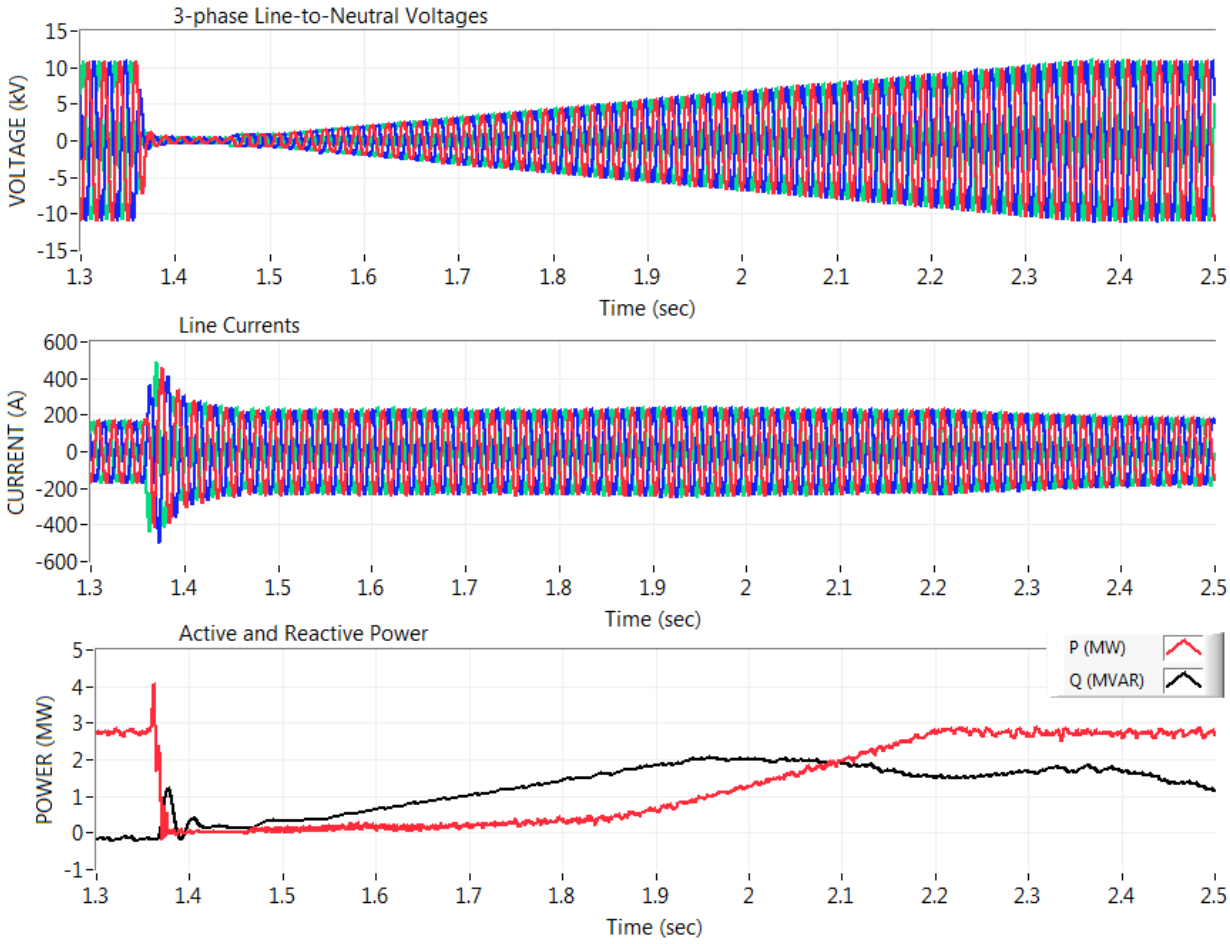

Figure 42. A three-phase voltage fault with slow recovery

5.3.4 Overvoltage Fault Testing under the Full Turbine Load

Overvoltage tests were conducted when the CGU transformer was set to the higher tap position. In this section, we show results for the single, two-, and three-phase overvoltage tests when GE turbine was operating at its rated 2.75-MW generation level. The CGI terminal voltages were commanded from their nominal 13.2-KV values to the 130% level (17.2 kV). Two recovery cases were emulated for all fault conditions: the fast-recovery case, when the CGI voltages were commanded back to their nominal prefault value in 100-ms interval and the slow-recovery case, when voltages were commanded to restore their nominal prefault level with slow 2- or 3-s ramping. The wind turbine was able to ride through fast-recovery overvoltage faults. It was tripping off during the slow-recovery 130% faults, but was able to ride through the 120% faults with slow recovery. For this reason, we include results for the 130% overvoltage tests only for the fast-recovery cases. The graphs for the single, two-, and three-phase 130% and 120% overvoltage faults for the fast- and slow- recovery conditions are shown in Figure 43 to Figure 48. As in the low-voltage testing case, the CGI acts as a stable voltage source for all symmetrical and nonsymmetrical conditions independently on wind turbine dynamics.

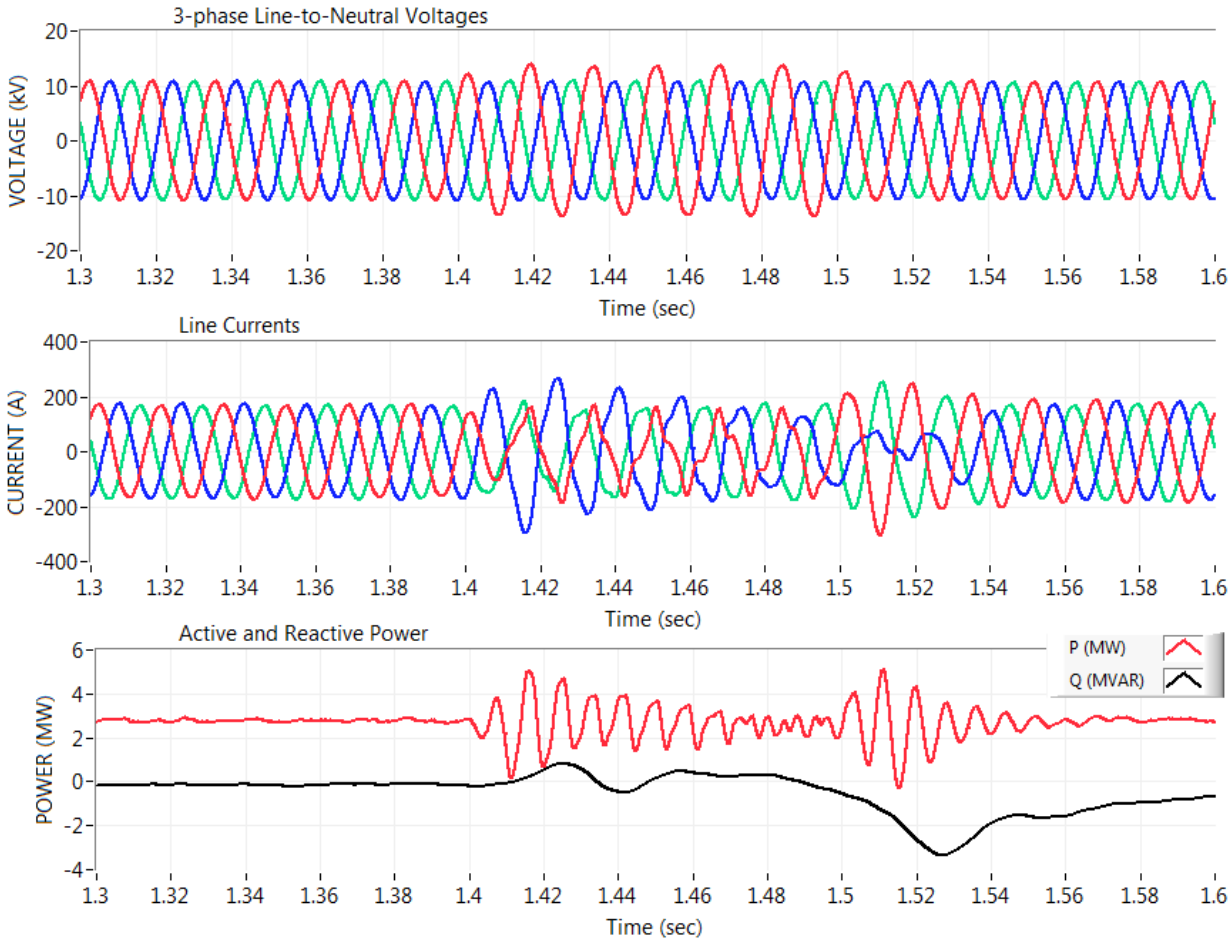

Figure 43. A single-phase 130% overvoltage test with fast recovery

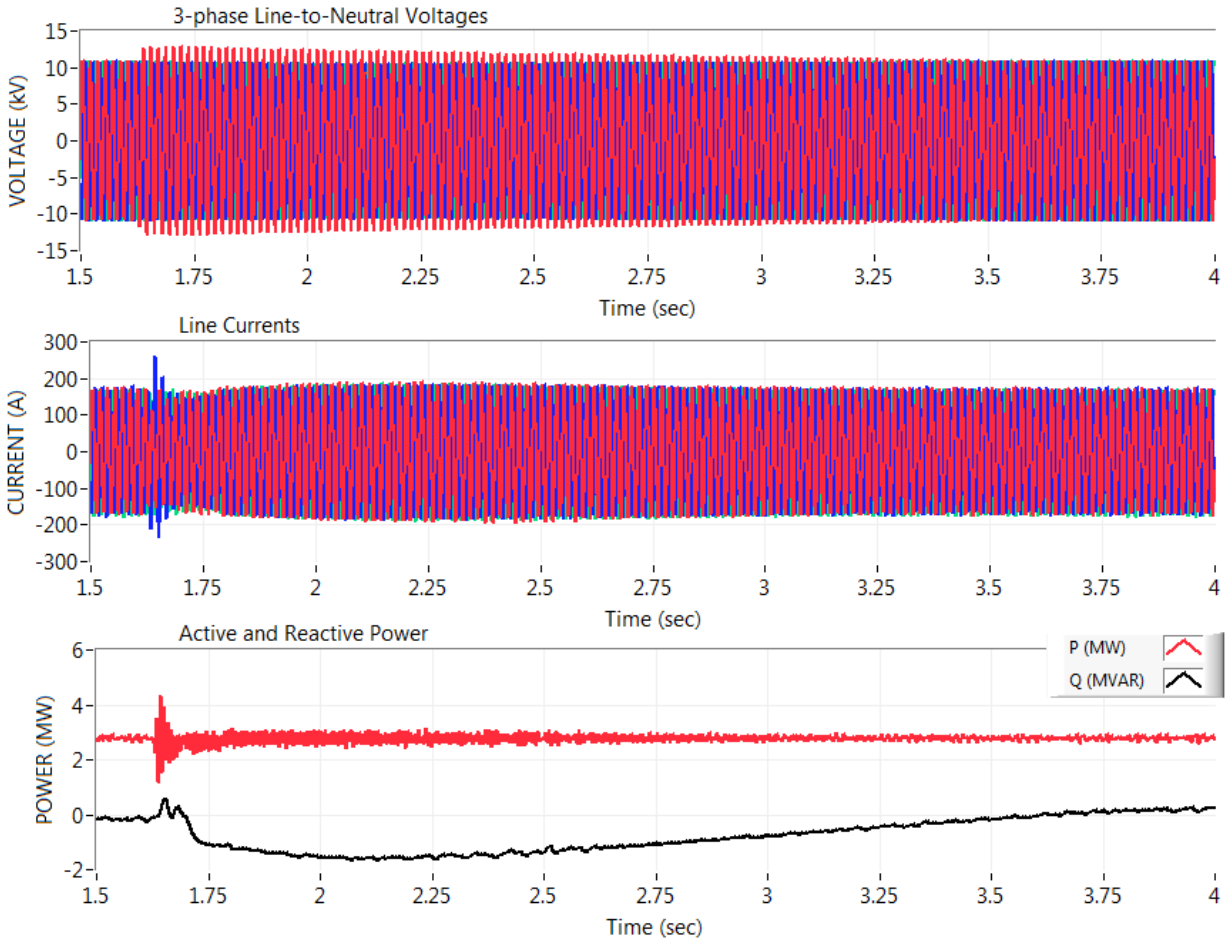

Figure 44. A single-phase 120% overvoltage test with slow recovery

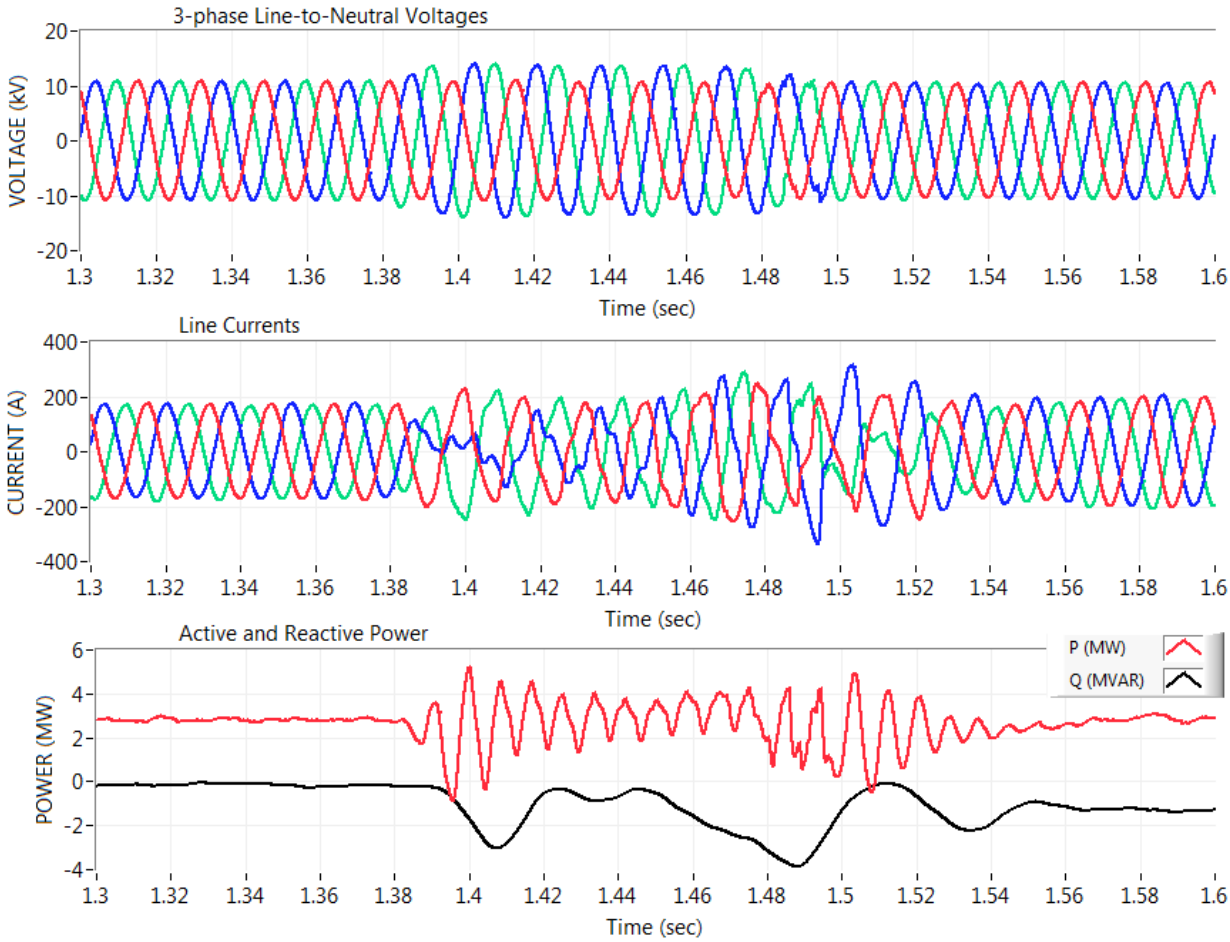

Figure 45. A two-phase 130% overvoltage test with fast recovery

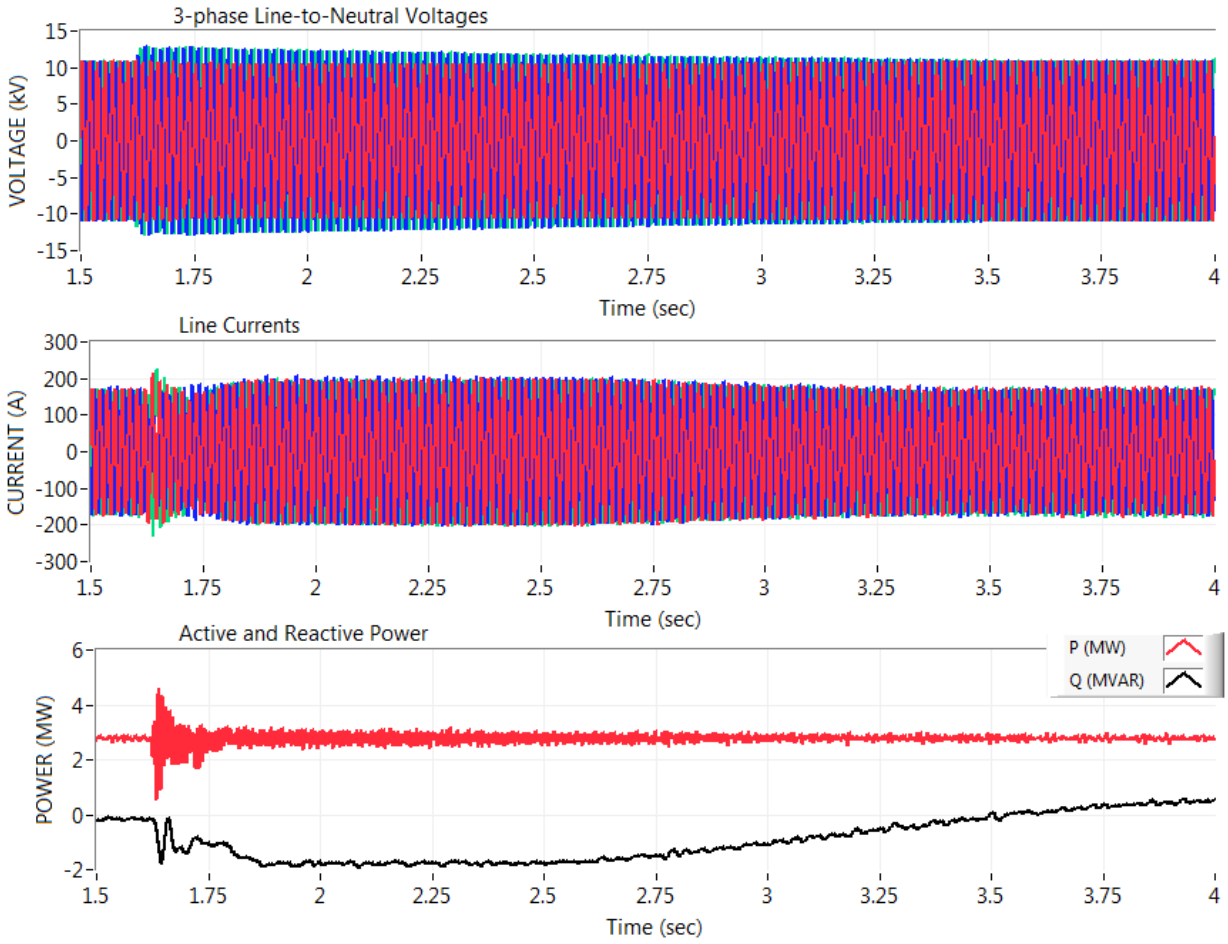

Figure 46. A two-phase 120% overvoltage test with slow recovery

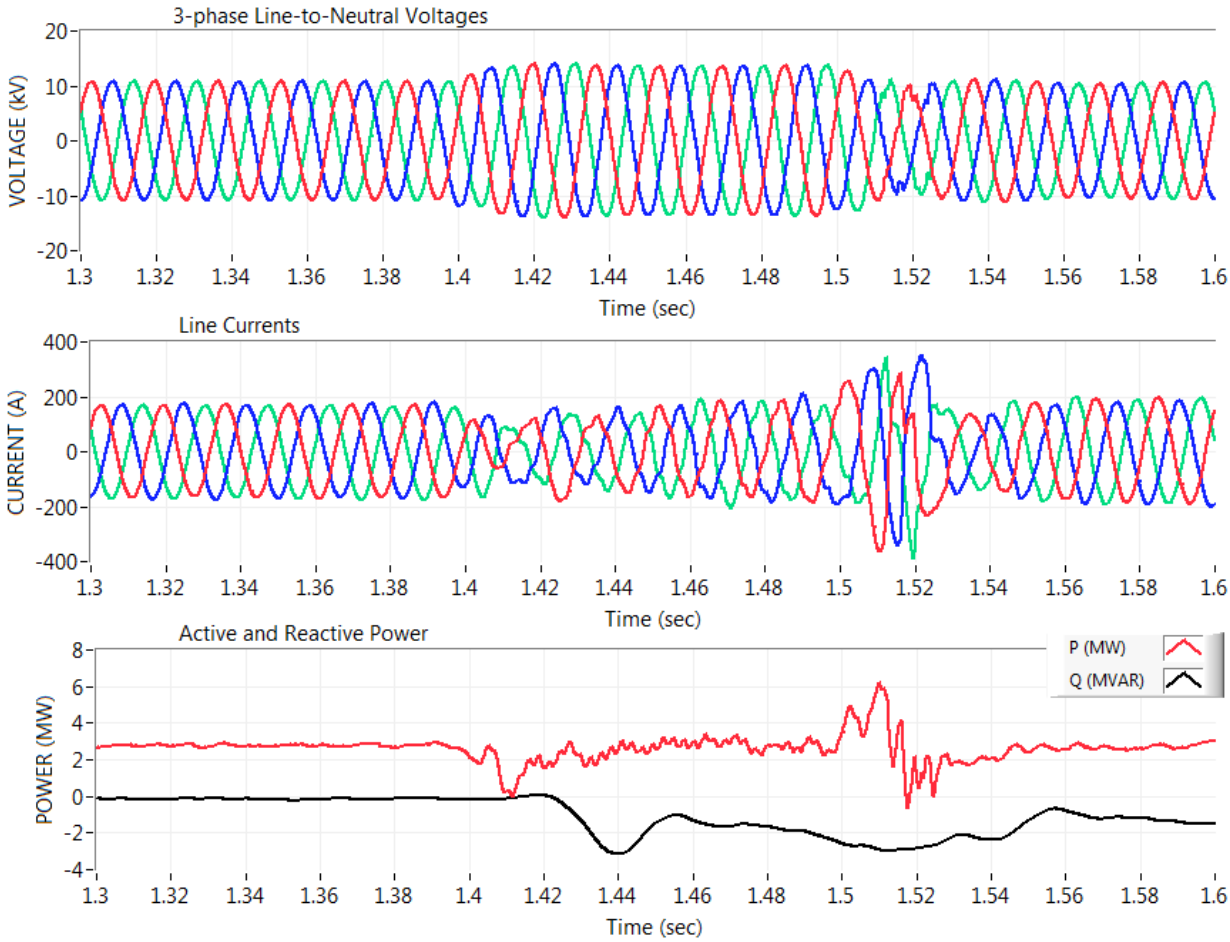

Figure 47. A three-phase 130% overvoltage test with fast recovery

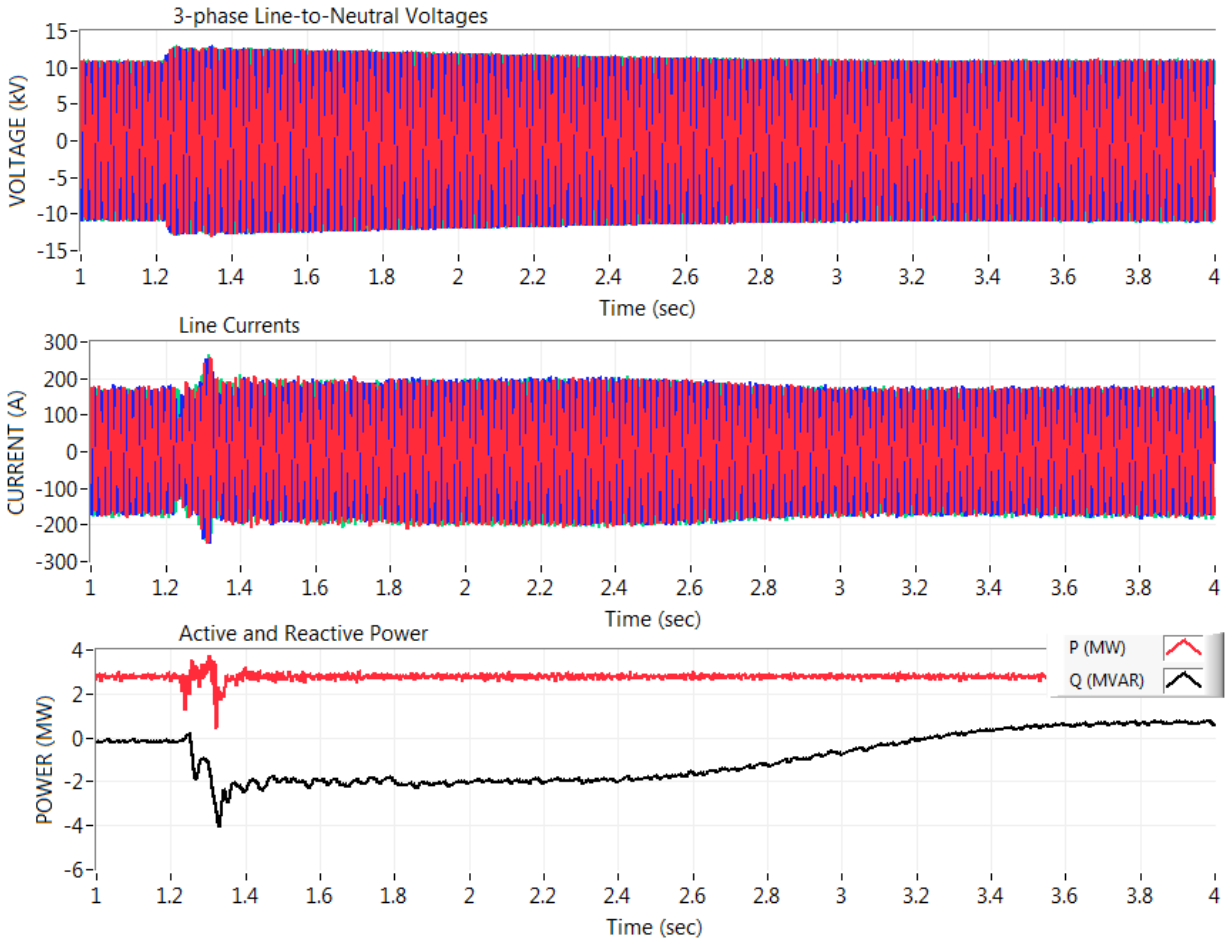

Figure 48. A three-phase 120% overvoltage test with slow recovery

5.4 CGI Frequency Tests

The CGI's ability to control the frequency of voltage on its 13.2-kV bus was tested under load when operating the GE 2.75-MW generator. The purpose of this test was to verify that the CGI can replicate real frequency excursions that have been measured in various power systems. Figure 47 shows the result of a test that emulates a frequency drop event that was measured in the U.S. Western Interconnection in 2011. This particular event was caused by a trip of a large power plant in the power system. In this example, we used the recorded frequency time series as a real-time frequency set point for the CGI controls. Figure 47 reveals that frequency voltage measured on the CGI terminals tracks this commanded frequency closely.

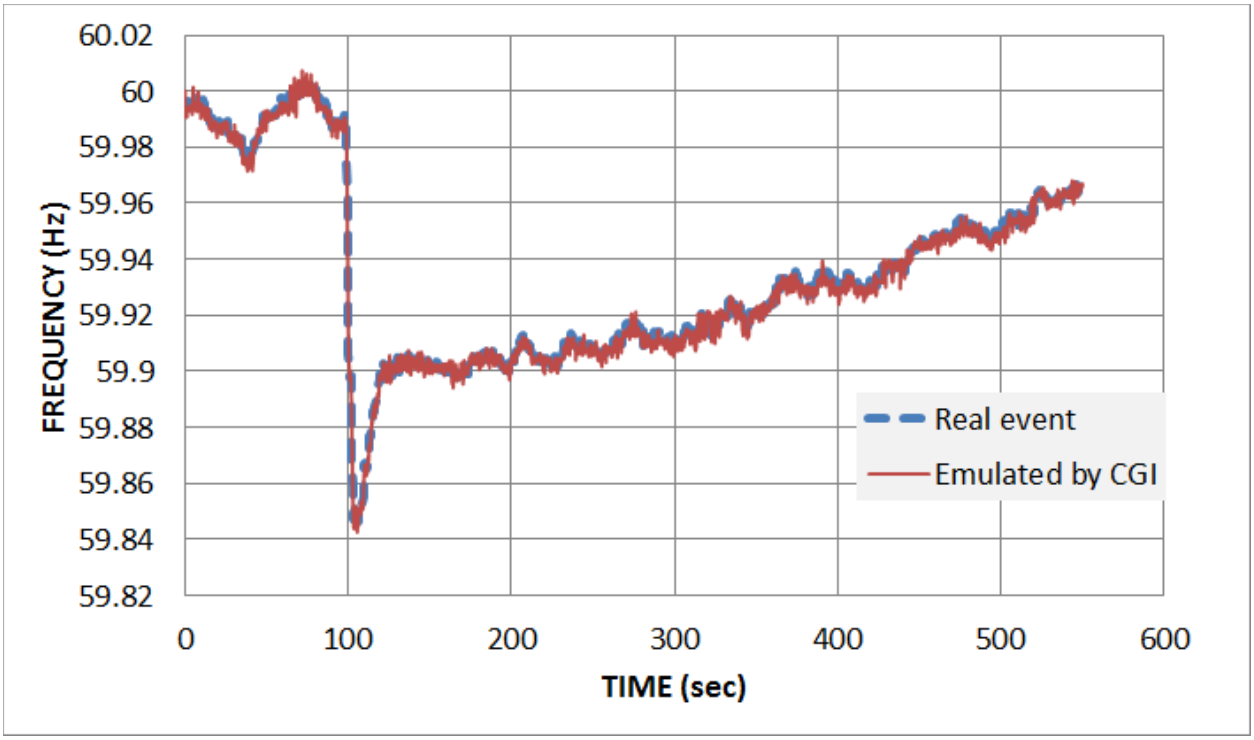

Figure 49. The CGI emulating a real frequency event from historic data

5.5 CGI Two-Turbine Test

The CGI's operation was tested under parallel operation with two NWTC dynamometers. First, the 750-kilowatt (kW) Gearbox Reliability Collaborative (GRC) turbine (on the 2.5-MW dynamometer) was accelerated to synchronous speed when its soft-starter activated to limit the inrush current. The start-up transients of the wind turbine (as measured on the CGI's 13.2-kV bus) are shown in Figure 50. The next step was to command the GRC generator to its full power (750 kW) as shown in Figure 51. Upon reaching the steady-state operation at 750 kW, the 2.75-MW GE wind turbine generator on the 5-MW dynamometer was synchronized with the CGI grid, then gradually (in 500-kW steps) brought up to its full power. At this point, the CGI was operating with two wind turbine generators connected to a simulated grid and producing 3.5 MW of combined real power. While absorbing this real power, the CGI was producing around 250 kilovolt amp reactive of reactive power as shown in Figure 52. As expected, the CGI demonstrated stable performance at the 3.5-MW load.

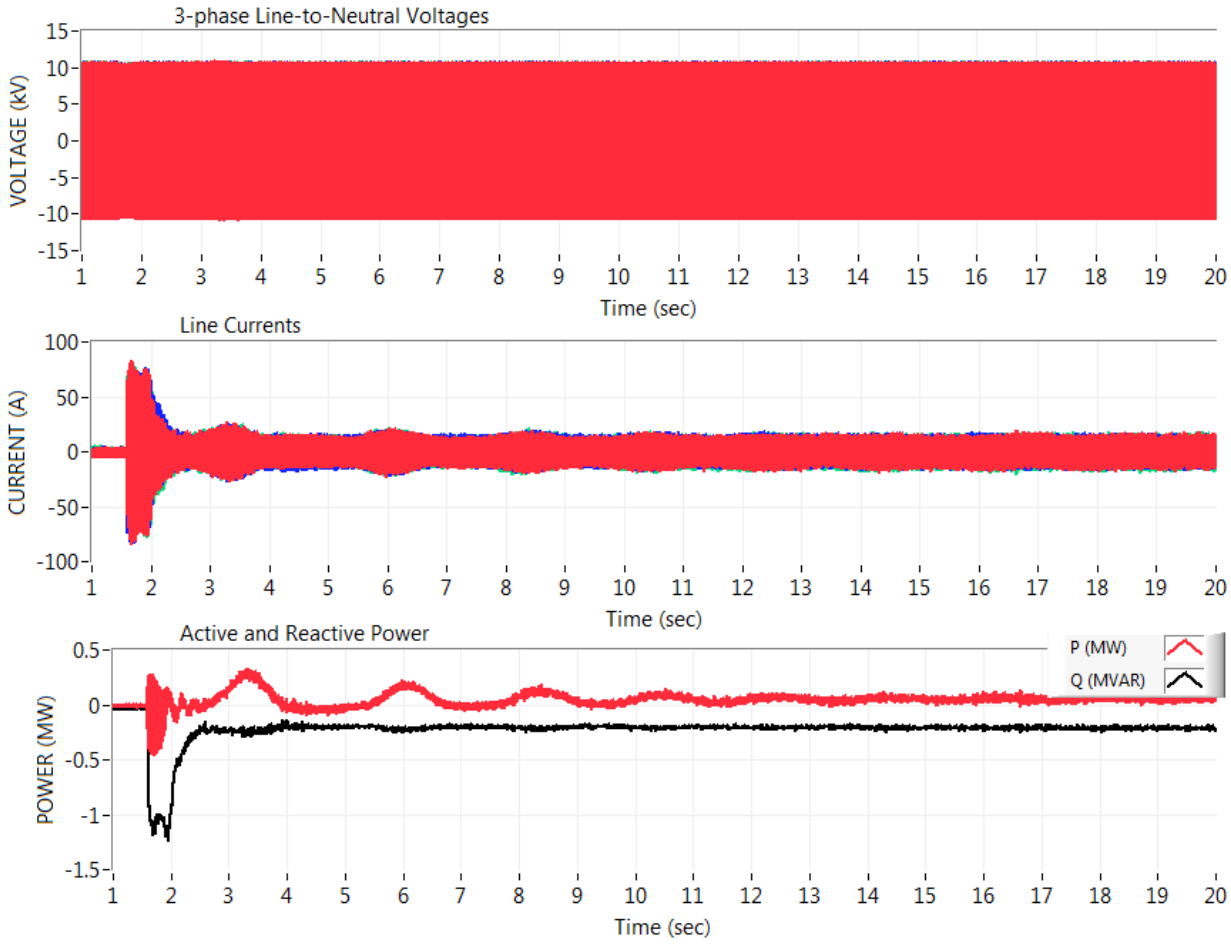

Figure 50. Start-up transients of the GRC's 750-kilowatt (kW) generator

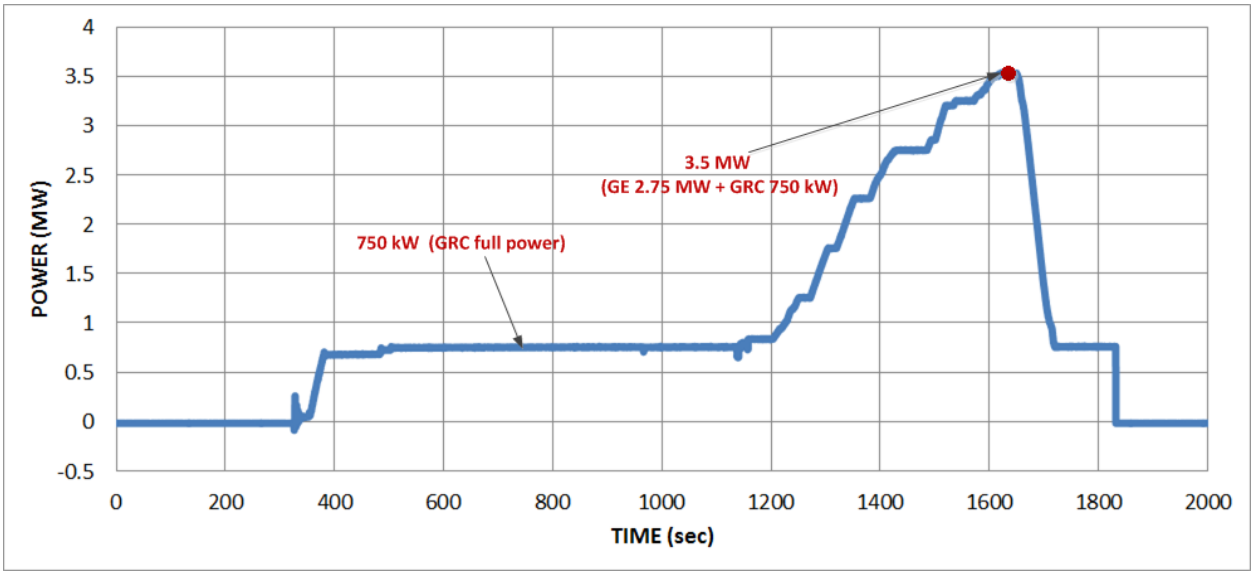

Figure 51. The CGI operating at the 3.5-MW load

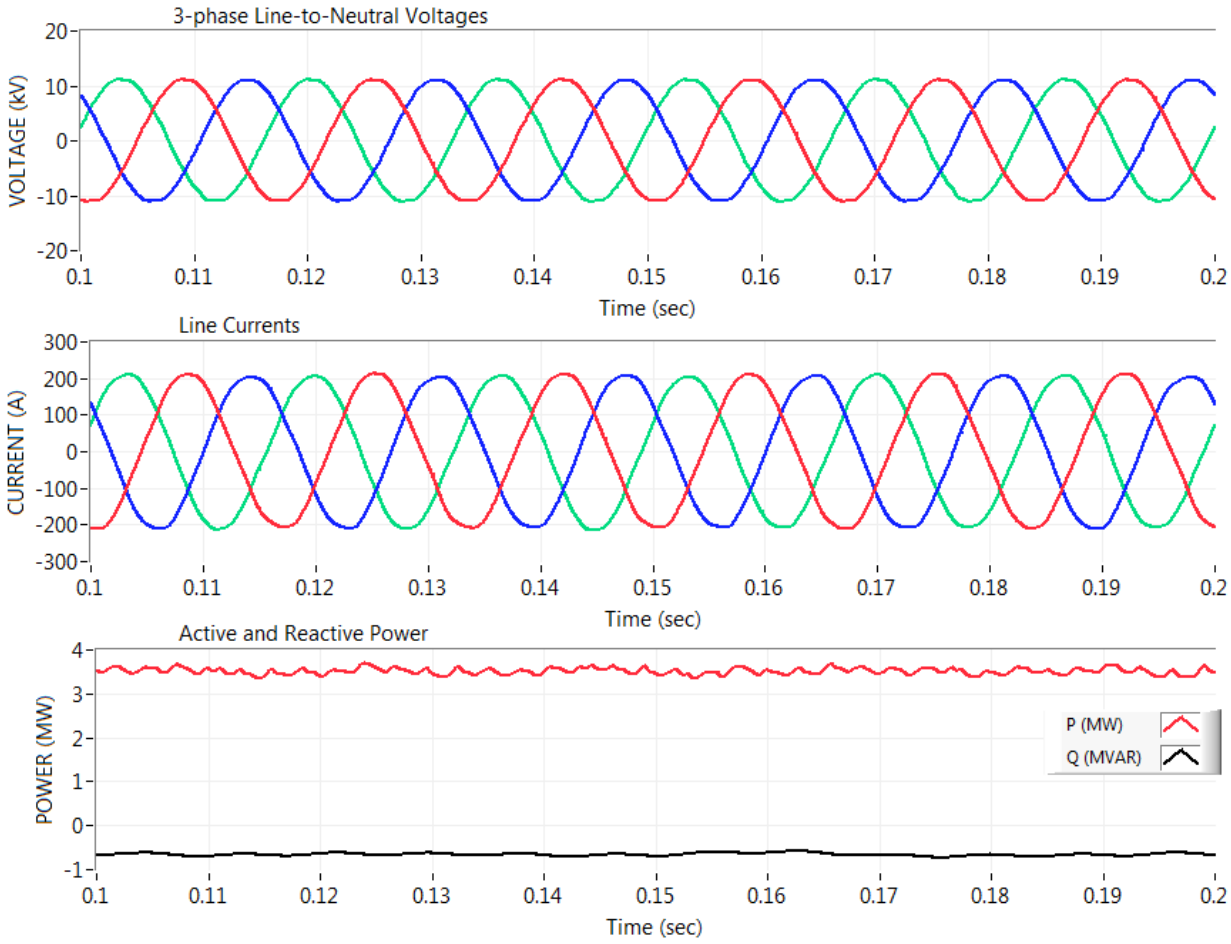

Figure 52. Current waveforms and power under the 3.5-MW load

6 Conclusions

A team of NREL engineers commissioned the 5-MW dynamometer facility and CGI through no-load and load testing of a GE 2.75 MW drivetrain over the course of several weeks in September 2013 and January/February 2014. These tests verified that the dynamometer motor and gearbox, NTL system and CGI can provide reliable and stable operation under both steady-state and transient conditions when operating with a test article. The dynamometer, NTL system and CGI met all of their design requirements and specifications when operating up to 2.75-MW load levels. The next steps for the dynamometer, NTL and CGI testing and characterization during fiscal years 2014 and 2015 include:

- Calibration of the LSS torque transducer
- Characterizing the additional and unmeasured NTLs that are applied to the test article arising from the LSS gear couplings
- Operating the CGI with a single field wind turbine installed at the NWTC (most likely the GE 1.5-MW machine provided by the U.S. Department of Energy)
- Operating the CGI with two NWTC field turbines in parallel.

Appendix A. Signal List

Table A-1. Baseline Dynamometer Data Channels

Location	Nomenclature	Expanded Nomenclature	Sensor
Dyno LSS	Tlss	Dynamometer low-speed shaft (LSS) torque	Strain gage
Dyno LSS	Ωlss	Dynamometer LSS speed	Encoder
Dyno LSS	Θlss	Dynamometer LSS azimuth	Encoder
NTL	NTL thrust	NTL thrust force	Calculated
NTL	NTL lateral	NTL lateral force	Calculated
NTL	NTL upward	NTL upward force	Calculated
NTL	NTL pitch	NTL pitch moment	Calculated
NTL	NTL yaw	NTL yaw moment	Calculated
NTL	NTL DX	NTL axial displacement	Calculated
NTL	NTL DY	NTL lateral displacement	Calculated
NTL	NTL DZ	NTL upward displacement	Calculated
NTL	NTL Θpitch	NTL pitch angle	Calculated
NTL	NTL Θyaw	NTL yaw angle	Calculated
Dyno LSS	Mlss uw 0-180	Dynamometer LSS upwind moment; gages at 0^o and 180^o	Strain gage
Dyno LSS	Mlss uw 90-270	Dynamometer LSS upwind moment; gages at 90^o and 270^o	Strain gage
Dyno LSS	Mlss dw 0-180	Dynamometer LSS downwind moment; gages at 0^o and 180^o	Strain gage
Dyno LSS	Mlss dw 90-270	Dynamometer LSS downwind moment; gages at 90^o and 270^o	Strain gage
Dyno LSS	DXlss uw 0	Dynamometer upwind flex coupling prox at 0^o	Displacement
Dyno LSS	DXlss uw 90	Dynamometer upwind flex coupling prox at 90^o	Displacement
Dyno LSS	DXlss dw 0	Dynamometer downwind flex coupling prox at 0^o	Displacement
Dyno LSS	DXlss dw 90	Dynamometer downwind flex coupling prox at 90^o	Displacement
NTL Flange	Mntlf 0-180	NTL flange moment gages at 0^o and 180^o	Strain gage
Location	**Nomenclature**	**Expanded Nomenclature**	**Sensor**

NTL Flange	Mntlf 90-270	NTL flange moment gages at 90° and 270°	Strain gage
Turbine Main Shaft	Mms 0-180	Turbine main shaft moment gages at 0° and 180°	Strain gage
Turbine Main Shaft	Mms 90-270	Turbine main haft moment gages at 90° and 270°	Strain gage
Test Stand	Mstnd E-W	Test stand moment gages at east and west	Strain gage
Test Stand	Mstnd N-S	Test stand moment gages at north and south	Strain gage
Test Stand	Tstnd yaw	Yaw torque	Strain gage
Dyno VFD	Wmotor	Motor actual speed	Encoder
Dyno VFD	Imotor	Motor actual current	Current transducer
Dyno VFD	Pmtr filtered	Motor power filtered	Calculated
Dyno VFD	Tmtr filtered	Motor torque filtered	Calculated
Dyno HSS	Tmtr shaft	Motor shaft torque	Torque transducer
Turbine Control	Pturbine	Test drivetrain power	Calc'd
Turbine Control	Ωturbine	Test drivetrain speed	Encoder
Dyno Motor	ACC mtr	Motor vibration	Accelerometer
Dyno Gearbox	ACC gbox	Gearbox vibration	Accelerometer
NTL	ACC ntl	NTL vibration	Accelerometer
Turbine Gearbox	ACC turb gbox	Turbine vibration	Accelerometer
Dyno Motor	Tmtr u1	Motor phase U1 winding temperature	Resistance Temperature Detector (RTD)
Dyno Motor	Tmtr v1	Motor phase V1 winding temperature	Resistance Temperature Detector (RTD)
Dyno Motor	Tmtr w1	Motor phase W1 winding temperature	Resistance Temperature Detector (RTD)
Dyno Motor	Tmtr u2	Motor phase U2 winding temperature	Resistance Temperature Detector (RTD)
Dyno Motor	Tmtr v2	Motor phase V2 winding temperature	Resistance Temperature Detector (RTD)

Dyno Motor	Tmtr w2	Motor phase W2 winding temperature	Resistance Temperature Detector (RTD)
Location	**Nomenclature**	**Expanded Nomenclature**	**Sensor**
Dyno Motor	Tmtr de	Motor DE bearing temperature	Resistance Temperature Detector (RTD)
Dyno Motor	Tmtr nde	Motor NDE bearing temperature	Resistance Temperature Detector (RTD)
Dyno Gearbox	Tgbox hss bearing	Gearbox HSS bearing temperature	Resistance Temperature Detector (RTD)
Dyno Gearbox	Tgbox oil return	Gearbox oil return temperature	Resistance Temperature Detector (RTD)
Turbine Gearbox	Tturb oil return	Turbine oil temperature	Resistance Temperature Detector (RTD)
Turbine Generator	Tturb gen	Turbine generator temperature	Resistance Temperature Detector (RTD)